Reference Definitions

1,***2***,***3***,***4***,***5***,***6***,***7***,***8***,***9***,***10***,***11***,***12***,***13***,***14***,***15***,***16***,***17***,***18***,***19***,***20***,***21***,***22***,***23***,***24***,***25***,***26***,***27***,***28***,***29***,***30***,***31***,***32***,***33***,***34***,***35***,***36***,***37***,***38***,***39***,***40***,***41***,***42***,***43***,***44***,***45***,***46***,***47***,***48***,***49***,***50***,***51***,***52***,***53***,***54***,***55***,***56***,***57***,***58***,***59***,***60***,***61***,***62***,***63***,***64***,***65***,***66***,***67***,***68***,***69***,***70***,***71***,***72***,***73***,***74***,***75***,***76***,***77***,***78***,***79***,***80***,***81***,***82***,***83***,***84***,***85***,***86***,***87***,***88***,***89***,***90***,***91***,***92***,***93***,***94***,***95***,***96***,***97***,***98***,***99***,***100***,***101***,***102***,***103***,***104***,***105***

Direct-Thermal Solar Hydrogen Production from Water Using Nozzles/Skimmers and Glow Discharge in the Gas Phase at Low Pressure and High Temperature

W.R. Pyle , M.H. Hayes, J.D. Healy, E.C. Petersen, A.L. Spivak, R. Cortez
H-Ion Solar Company, Richmond, California

Prepared for: K.L. Scholl and P.W. Koshak
National Renewable Energy Laboratory
U.S. Department of Energy
Golden, Colorado, USA

Task No. HY413801
Subcontract No. AAP-4-14240-01

Abstract

An investigation of direct-thermal solar hydrogen and oxygen production from water is described. Nozzle jets and skimmers have been used for separation of the products and suppression of recombination. The dissociation of water vapor and the separation of its products was conducted in plasma-enhanced, non-equilibrium glow discharges.

Summary

In this report we describe the status of our work with a **solar water dissociation** gas phase reactor:

Solar radiant energy was concentrated by a parabolic mirror to produce high temperatures on a nozzle inside a solar reactor fed with water vapor (steam) at low pressure, to produce hydrogen and oxygen by direct-thermal water vapor dissociation.

- A ceramic dissociator-nozzle was used as the target (absorber) for the concentrated solar-beam image. Water vapor was fed to the hot dissociator-nozzle by a feed-ring. Expansion of the water and its dissociation products into a lower pressure region was employed to relax vibrational and rotational oscillatory modes to provide quenching.

- A conical skimmer was used to separate the dissociated water vapor products, hydrogen and oxygen, from the unconverted water vapor in the expanding dissociator-nozzle jet. The objective was to separate the hydrogen and oxygen products from each other before they recombine back to water vapor.

- The dissociator-nozzle was operated with an electrical glow discharge at the water vapor feed inlet. In this way the steam flow field, where the radiation and convection heat transfer takes place, was populated with free electrons, ions and molecules in the excited state. The radiation absorption capture cross-section for water vapor was altered by the plasma glow discharge. Plasma glow discharge was used to enhance heat transfer between the nozzle surface and the water vapor molecules entering the nozzle.

- The product gas stream (containing hydrogen, oxygen and water) from the dissociator-nozzle's exhaust jet flow field was operated in a glow discharge. The purpose was to promote cata-phoretic segregation (separation) of the ionized and kinetically excited states in the water vapor and products. This affects the nozzle plume flow-field between the dissociator-nozzle jet and a conical-skimmer. The expanding jet flow-field downstream of the dissociator-nozzle separates the water decomposition products spatially, enriching the core of the jet flow-field with the heavier oxygen and water, and enriching the peripheral flow-field with the lighter hydrogen. Transverse diffusion of hydrogen appeared to be responsible for separation, as the product gas stream expanded to form a shock wave, falling from supersonic to subsonic velocity.

- Progress to date includes:

  a) Operation of the reactor for over 50 hours on-sun at 2600-2900 K nozzle surface temperature without failure of materials.

  b) Selection of reactor materials and geometry capable of sustaining a glow-discharge under on-sun conditions, without extinction, for over 50 hours.

  c) Dissociation of water and separation of hydrogen at 1 to 2 % overall efficiency (solar to hydrogen.)

Introduction

A sustainable, non-polluting energy currency is required to provide for human needs such as cooking, heating, transportation, electricity production, and refrigeration. An economically viable method for producing large quantities of hydrogen from water using sun-light would satisfy this need, in a "Hydrogen Economy".

Solar hydrogen production and utilization does not create undesirable environmental side effects, since the cycle is a closed cycle. Water is converted to hydrogen and oxygen during production, followed by conversion back to water during utilization. The solar energy each day is stored in the chemical products of water dissociation for later utilization.

Pioneering studies of solar hydrogen and oxygen production from water occurred throughout the world during the 1970's and early 1980's as a response to the oil shocks of 1973 and 1978/1979. After a lull in activities during the mid and late 1980's, interest in direct water dissociation and other hydrogen production technologies has again increased during the early 1990's due to increasing environmental problems. Renewed interest in solar hydrogen production has also been influenced by fuel cell advancements and solar concentrator developments [1].

Water Dissociation to Produce Hydrogen and Oxygen

Our research objective is to develop a process that can attain a high level of water vapor dissociation and efficiently separate the hydrogen from the oxygen and un-converted water vapor.

At high temperatures, above about 1800 K, water vapor (steam) begins to dissociate into a mixture of H_2, O_2, H_2O, O, H and OH. The extent of dissociation increases with increasing temperature and decreasing pressure. The water and the diatomic hydrogen and oxygen species completely dissociate into H(atomic hydrogen) and O (atomic oxygen) above about 3500 K under equilibrium conditions at 1 mm Hg absolute pressure.

An equilibrium diagram for water vapor and its dissociation products, as a function of temperature, is shown in Figure 1 below [2-6]:

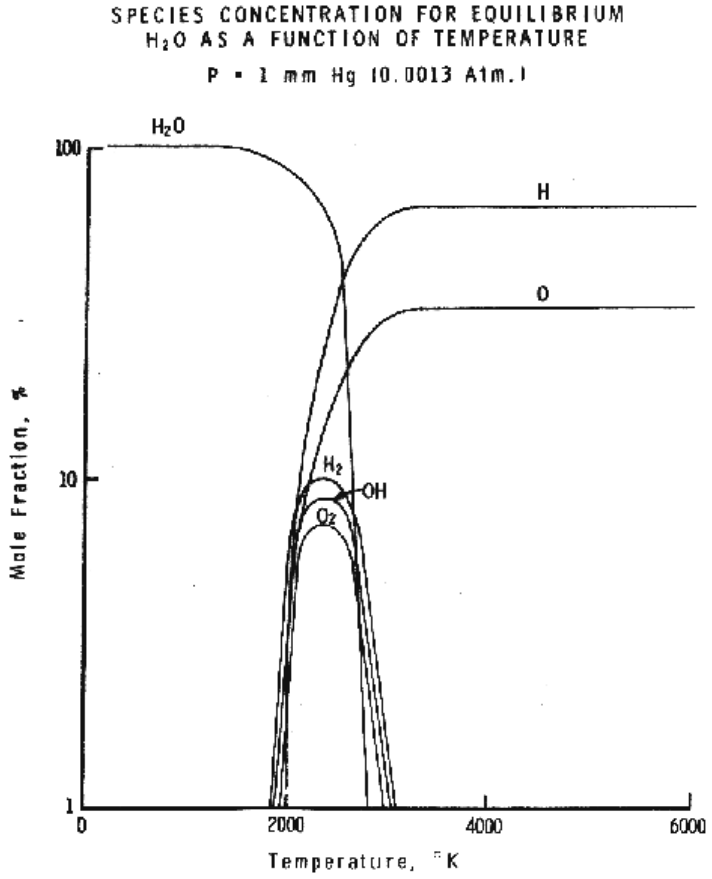

Figure 1

Pressure influences the equilibrium for the water dissociation reaction as shown in Figure 2.

Figure 2

By operating our process under non-equilibrium conditions, greater yields of the hydrogen and oxygen products are sought at lower reactor wall temperatures.

Reduction of the total pressure may have an unexpected advantage. By reducing the amount of water which must be processed to achieve a given amount of hydrogen and oxygen production, low pressure operation reduces irreversibility associated with every stage of the process [7].

There is a trade-off between the increased pumping work expenditure to achieve lower pressures, and the increased dissociation of water to hydrogen and oxygen, which the lower pressure promotes(Figure 2). Pumping work requirements should be minimized to reduce parasitic power losses which lower the process efficiency while allowing reasonable product throughput. This requires that the pressure ratio across the nozzles in the reactor not be excessive, and the total pressure not be too low in the separator section.

Endothermic Water Vapor Dissociation Reactions

Endothermic reactions can be carried out with the aid of electricity, as in electrolysis. However, thermal power from concentrated solar radiation can be used without any mechanical or electrical input and without the aid of any catalyst to achieve water dissociation. The direct thermal method has two advantages: it is very simple in its principle and it is versatile and adaptable to many endothermic gas phase reactions. This method does not suffer from the corrosive reagent problems of various multi-step lower temperature thermo-chemical cycles. New problems arise, however, in finding reactor materials capable of withstanding the higher temperatures required with one-step concentrated radiation water thermolysis. The materials used in the reactor must be capable of withstanding the thermal cycling and shock brought about by the intermittent nature of solar diurnal and weather cycles.

The chemical reactions associated with high temperature dissociation of water vapor are shown below, along with their pressure equilibrium constants:

Chemical Reactions

$$H_2O \rightarrow H_2 + 1/2O_2 \quad (1)$$

$$H_2 \rightarrow 2H \quad (2)$$

$$O_2 \rightarrow 2O \quad (3)$$

$$O + H \rightarrow OH \quad (4)$$

Pressure Equilibrium Constants

$$K_1 = XH_2\sqrt{P * XO_2} / XH_2O$$

$$K_2 = P * X^2H / XH_2$$

$$K_3 = P * X^2O / XO_2$$

$$K_4 = XOH / (P * XO * XH)$$

Mole Fraction Equation

$$XH_2O + XH_2 + XH + XO_2 + XO + XOH = 1$$

P = Total Pressure

X = Mole Fraction

Water vapor dissociation has an activation energy threshold of about 135 kcal/mole (5.9 electron volts). Atomic hydrogen and oxygen are formed and then recombined to diatomic hydrogen and oxygen, losing about 78 kcal/mole in the recombination process. The reverse reaction occurs during ignition and combustion. See Figure 3.

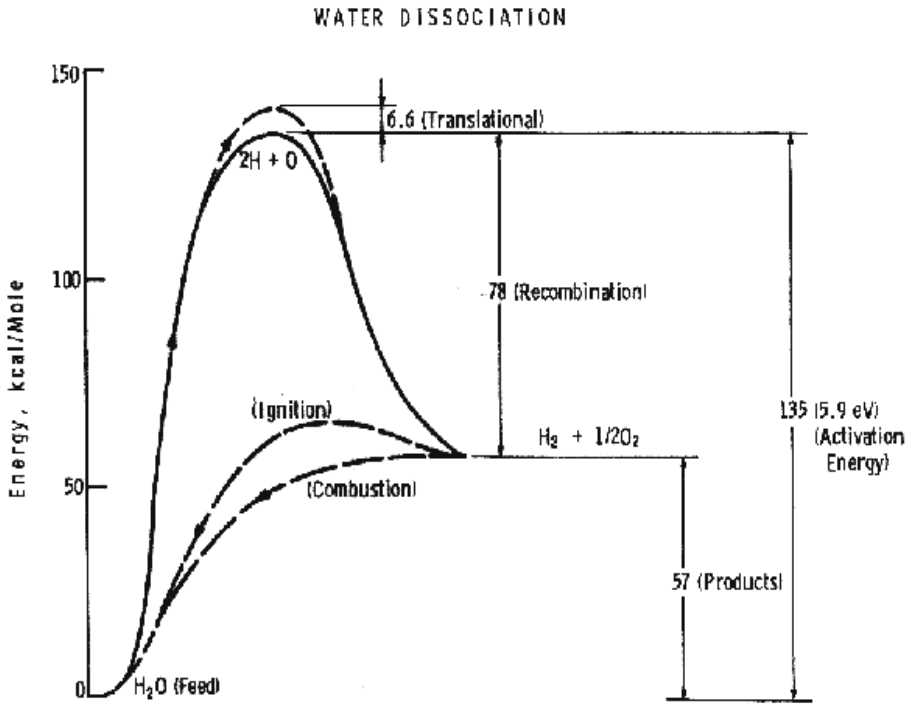

Figure 3

Non-equilibrium plasma-chemical reactions associated with water vapor glow discharges

The process of decomposition of water in the plasma state can be accomplished at highest efficiency where the electron temperature is not sufficient for intense excitation of the electron states, and the larger portion of the electron's energy contributed to the discharge is expended for excitation of vibration modes and for dissociative attachment [8-12]

Dissociation of water vapor by vibrationally excited states of the molecule is accomplished by successive stages of water oscillative excitation, population of highly excited states during the V-V relaxation and, finally by reactions with participation of H_2O^* (where the * denotes the vibrationally excited state of water) [8]. The reaction is initialized in the bimolecular act:

$$H_2O^* + H_2O^* \Rightarrow H + OH + H_2O$$

The radicals H and OH initiate a reaction with participation of the oscillatively excited molecules:

$$H + H_2O^* \Rightarrow H_2 + OH$$

$$OH + H_2O^* \Rightarrow H + H_2O_2$$

Water decomposition by dissociative attachment requires that in each reaction an electron disappears and a negative ion is produced. Plasmochemical dissociative attachment reactions become energetically effective when each electron produced in the plasma can repeatedly participate in the dissociative attachment process. Multiple use of the electron becomes possible due to a high rate of negative ion collapse by electron impact [8]. The chain process initializes:

$$e + H_2O \Rightarrow H^- + OH$$

$$H^- + e \Rightarrow H + e + e$$

Termination of the chain results from recombination with water and OH in a three-body collision:

$$H + OH + H_2O \Rightarrow H_2O + H_2O$$

The parallel channel of the chain extension has poorer kinetics because of a higher activation barrier of the limiting process [8]:

$$OH + H_2O \Rightarrow H_2 + HO_2$$

$$HO_2 + H_2O \Rightarrow H_2O_2 + OH$$

The total efficiency of the process depends on the energy losses in the discharge, the efficiency associated with the negative contribution of the chain-breaking reaction, the heat losses of the excited-state reactions, and finally on the efficiency of the reaction relative to the oscillative relaxation. The energy transfer efficiency of vibrational excitation by electron impact is a function of the energy contribution to water: oscillations, translational motion, rotation, and dissociative attachment. The energy transfer efficiency of the chain process depends on the chain length. When the chain length is 100 (and there are 100 consecutive initialization reactions by electron capture before a three-body recombination and chain termination), the chemical efficiency may approach 85%. Whereas, in the absence of a chain process (chain length = 1) the chemical efficiency may be only 50% [8].

Separation Methods for Removing Hydrogen/Oxygen from Water Vapor

Various methods for separating hydrogen and oxygen from partially dissociated water vapor have been proposed and some have been experimentally investigated. Some of the separation schemes are:

- Quenching with an inert gas
- Effusion Membranes (Knudsen flow regime)
- Diffusion Membranes
- Semi-permeable Membranes
- Solid Electrolytes (Ionic Conductors or Ionic/Electronic Mixed Conductors)
- Jet Separators (Nozzles/Skimmers)
- Cyclone and gas centrifugal separators
- Magnetic (oxygen is paramagnetic and can be influenced by a magnetic field.)
- Electric (hydrogen and oxygen positive and negative ions are influenced by electric fields)
- Rotating plasma (crossed electromagnetic fields)
- Microwaves
- Ultrasonic

An international effort has been directed toward the use of concentrated solar energy in obtaining hydrogen and oxygen from water. In France researchers expanded the theoretical and experimental understanding of quenching separations (using cold gas jets) and membrane separations (using solid oxide electrolytes) on dissociated water vapor [14-26]. In the USA solar reactors using effusion membranes, cyclone separators, jet separators and the absorption and emission characteristics of diffuse enclosures were studied [7,13,27-36]. Canadian researchers investigated high temperature solar reactor designs for hydrogen production, water quenching, and low temperature diffusion separations [37-43]. In Israel solar water thermolysis reactor designs were analyzed and tested [44-46]. In Japan, theoretical investigations of direct water splitting and two-step water splitting reactions were conducted [47-49]. In Russia plasma-chemical water splitting cycles were proposed and tested [8,9-12].

In this paper we investigate jet separators and plasma enhanced dissociation and separation of water vapor in non-equilibrium glow discharges.

Dissociator-Nozzle Application to Production of Hydrogen and Oxygen from Water Vapor

A block diagram of the Photo-separatory Nozzle reactor [32] and the process under investigation is shown in Figure 4:

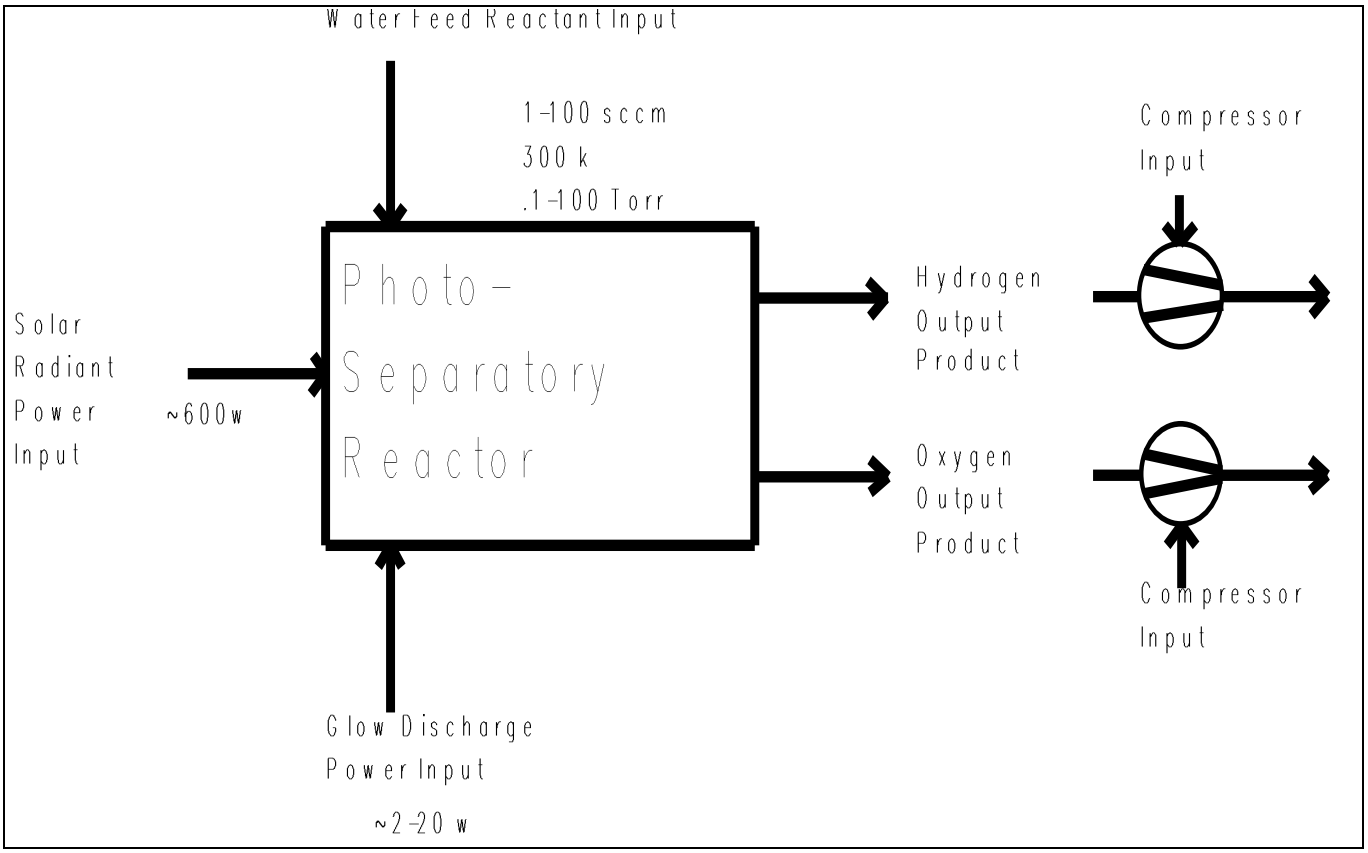

Figure 4
Block Diagram of Photo-separatory Reactor

Concentration and Absorption of Sunlight in Solar Reactor

Sun-light was concentrated using a 152cm (60 inch) parabolic mirror and directed through the entrance window of a high-temperature gas-phase reactor. Inside the solar reactor the concentrated radiant energy was focused onto a trumpet-shaped ceramic dissociator-nozzle. See Figure 5. An optical pyrometer with a video camera looks through a prism and a hole in the concentrator mirror, then through the quartz reactor window to view the dissociator-nozzle surface and obtain nozzle surface temperatures.

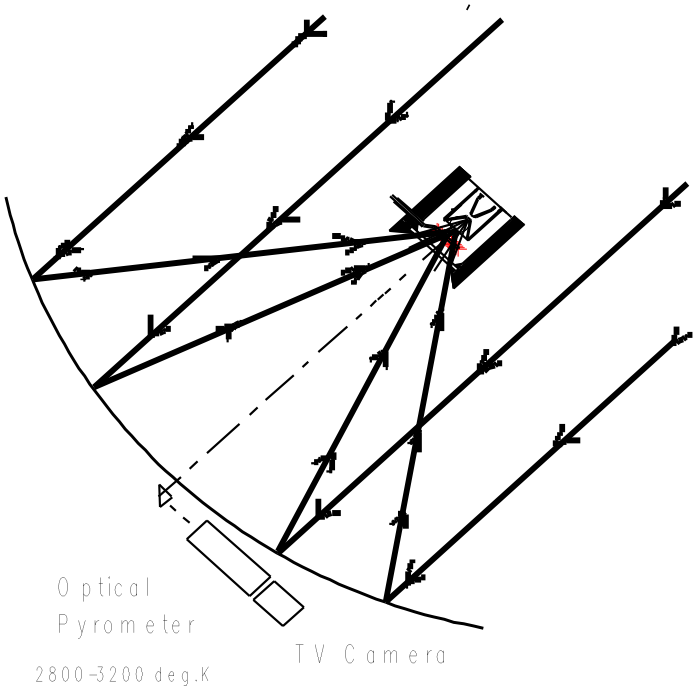

Figure 5
Solar Reactor at Focal Point of Parabolic Mirror Concentrator

The solar spectrum at sea level, on Earth with air mass of 1, and in space with air mass of zero, is depicted in Figure 6 [50]. Note the water vapor absorption which occurs as the light is passing through the atmosphere. This absorption severely limits the energy spectrum available for water dissociation at the earth's surface. Thus the need for plasma enhancement of gas heat transfer from a hot surface reaction site.

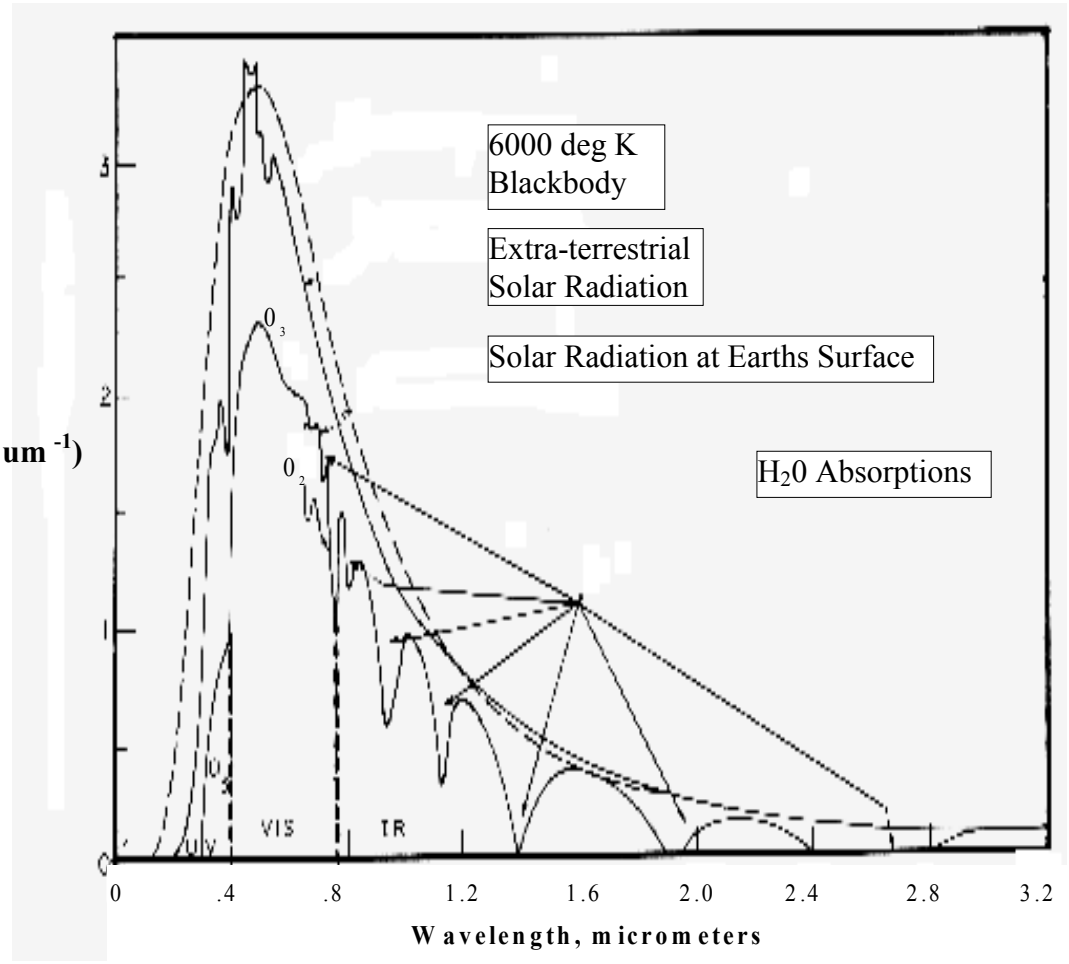

Figure 6
Solar Spectrum at Sea Level on Earth and in Space

Solar heat source temperature can be calculated as a function of the concentrator optical concentration ratio, reflection coefficient, and arriving solar power density as shown below:

Solar Heat Source

$$T = \sqrt[4]{(\alpha * N_r * S_i * C) / \sigma}$$

Where:

T = degrees Kelvin

α = Heat Conversion Efficiency($\approx$ 0.8 for ceramic surface)

N_r = Reflection Coefficient ($\approx$ 0.9 for front surface mirror)

S_i = Density of Incident Solar Energy (0.6 - 1.2 kW / m^2)

C = Concentration Ratio (area of mirror to image area)

σ = Stefan - Boltzman constant

Reflected light from the reactor chamber window is significant, but neglected and taken as 0% in this analysis.

Solar Collection Efficiency

$$N_c = \frac{(I * A * N_o * \alpha - a * \varepsilon * \sigma * T^4)}{I * A}$$

Where:

I = Insolation

A = Collector area

N_o = Optical efficiency

a = Aperture area

ε = Emissivity

α = Absorptivity

σ = Stefan - Boltzman constant

T = Temperature

Figure 7 is a plot of solar collection efficiency versus temperature at various concentration ratios. To efficiently capture solar radiant energy at high temperatures, very high concentration ratios are needed (>10,000). The recent development of two stage concentrators may help lower the cost of achieving concentration ratios in this range [1].

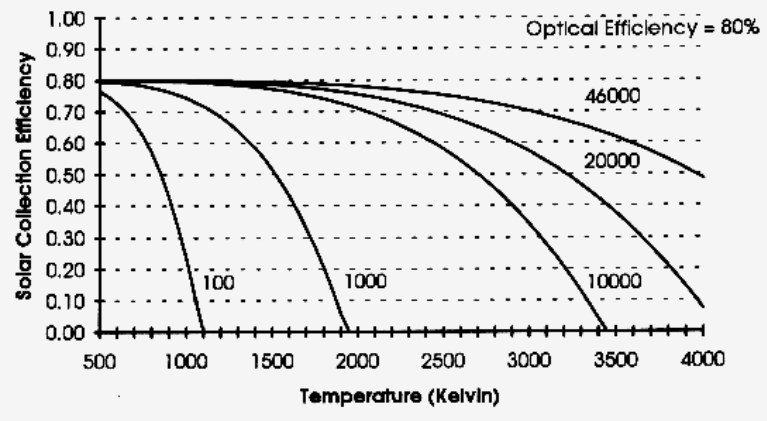

Figure 7
Solar Collection Efficiency versus Temperature

The radiation absorption cross-section for water vapor is not well matched to the visible spectrum of sunlight at the earth's surface, however, as shown in Figure 8 [51]. The radiation absorption cross-section for water vapor is better matched by the solar spectrum in space (Figure 6.)

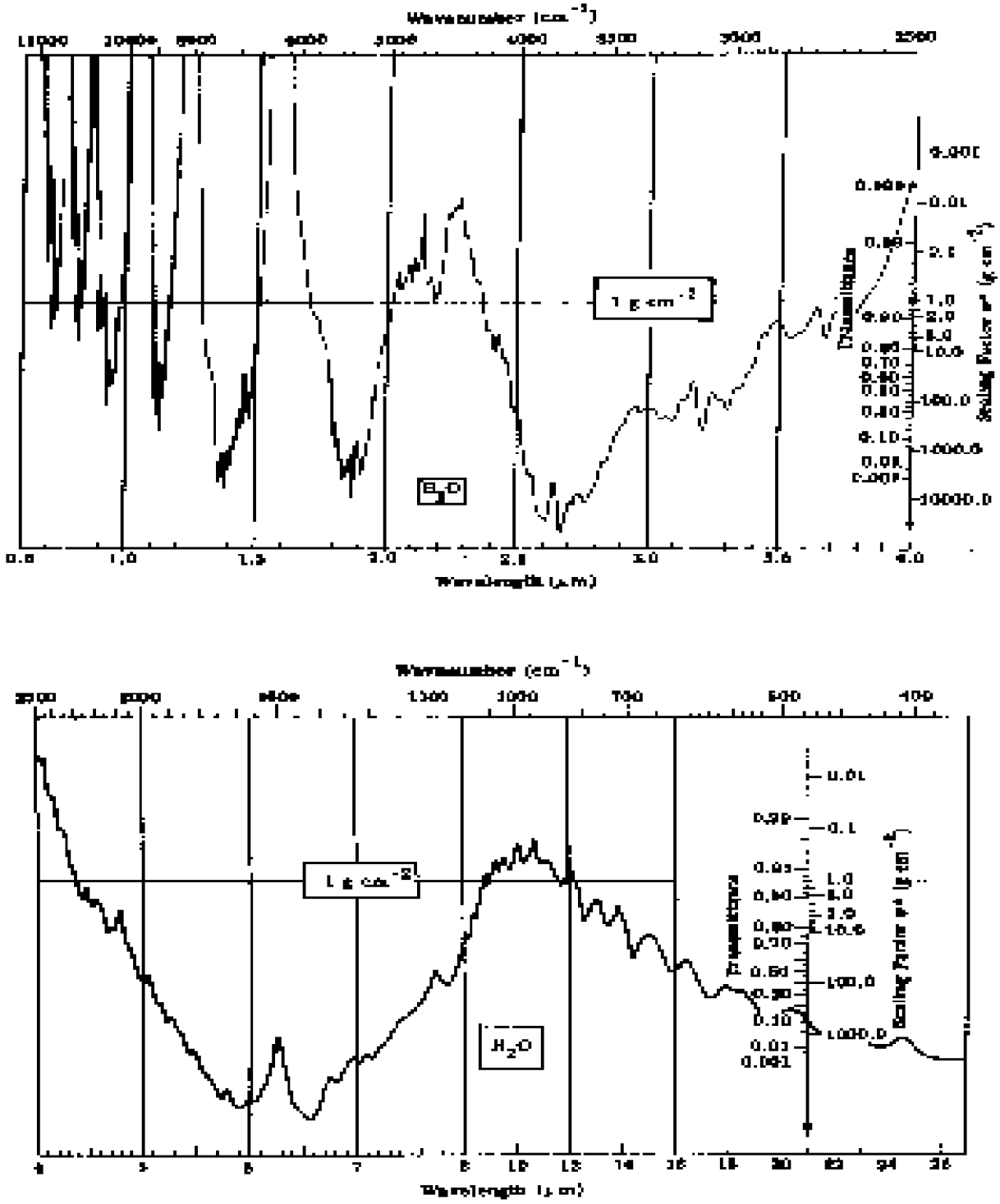

Visible and infrared transmittance of water vapor, used in atmospheric modeling. (From *The Infrared Handbook*, Office of Naval Research, p. 5-56)

Figure 8
Water Vapor Transmission Versus Wavelength

Radiant surface heating of the dissociator-nozzle provides the driving force for chemical reactions. Electron and ion energy drives reactions in the plasma. Gas-phase absorption reactions do not contribute the dominant driving force in the visible and infra-red portions of the spectrum. Gas phase absorption reactions are more important in the infrared portion of the solar spectrum. However, as gas pressure is reduced, path length is reduced, and as temperature is increased, the water vapor absorptivity at all solar wavelengths is greatly diminished [52].

Re-radiation from the surface of the hot trumpet-shaped dissociator-nozzle causes "down-shifting" of the visible and infrared spectrum according to the Planck distribution as shown in Figure 9 [53]. If the process occurs inside a black body cavity with the radiation introduced through a small aperture behind the quartz window, the absorptance of the working fluid, water, and its dissociation products may be unimportant. The heat transfer parameters would be associated with the geometry and mechanics of the apparatus [7].

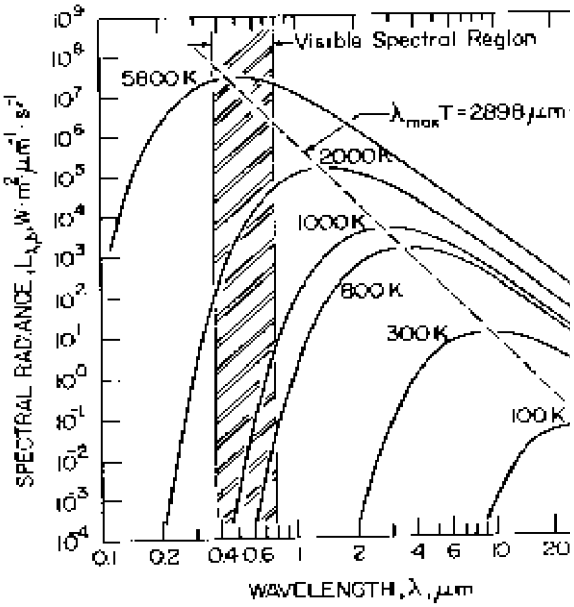

Figure 9
Spectral Radiance of a Black Body at High Temperatures

Water vapor was delivered to the hot surface of the dissociator-nozzle by means of a feed-ring. See Figure 10.

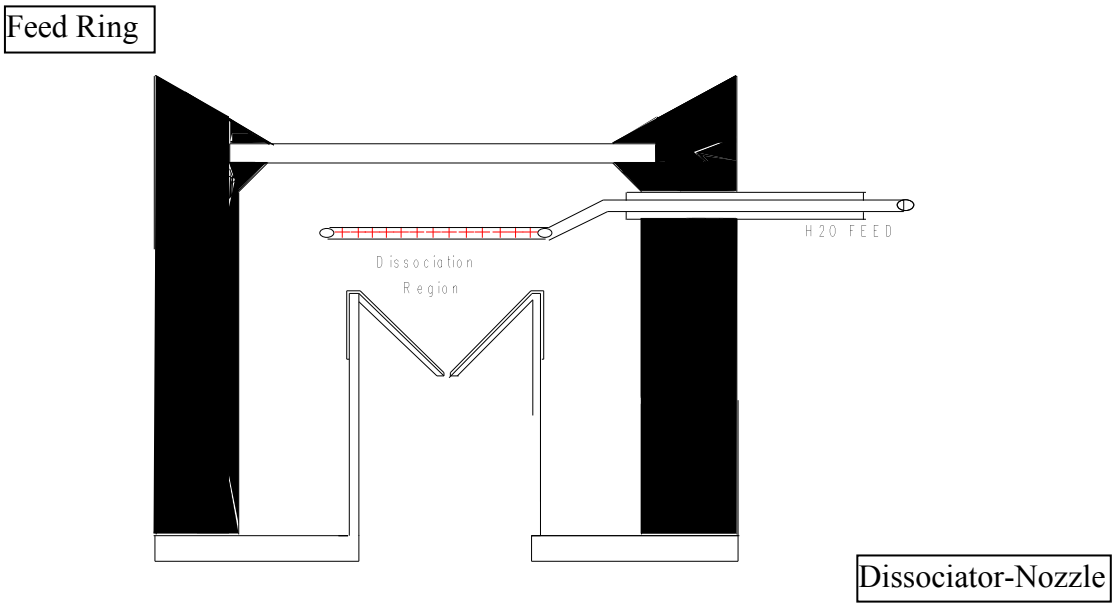

Figure 10
Solar Reactor with Dissociator-Nozzle and Water Vapor Feed Ring

By raising the temperature of the nozzle surface to a sufficiently high value (using the nozzle as a target for concentrated sunlight) and dropping the water vapor pressure to a sufficiently low value, we are attempting to produce significant water vapor dissociation. Systems which continuously remove the evolved hydrogen and oxygen can produce more product gases from water vapor at a lower temperature according to Le Chatlier's principle. The pressure inside the nozzle tube must be lower than on the outside (dissociation region) to cause the driving force for sonic flow through the nozzle throat (pressure ratio > 0.55) to produce a jet and shock-wave down stream.

Glow-Discharge Enhancement of Radiation and Convection Heat Transfer

In this investigation we are studying the non-isothermal low-pressure glow-discharge region shown in Figure 11.[13] It can be seen that the enthalpy change may be greater than the water dissociation activation threshold of 135 kCal/mole(5.9ev).

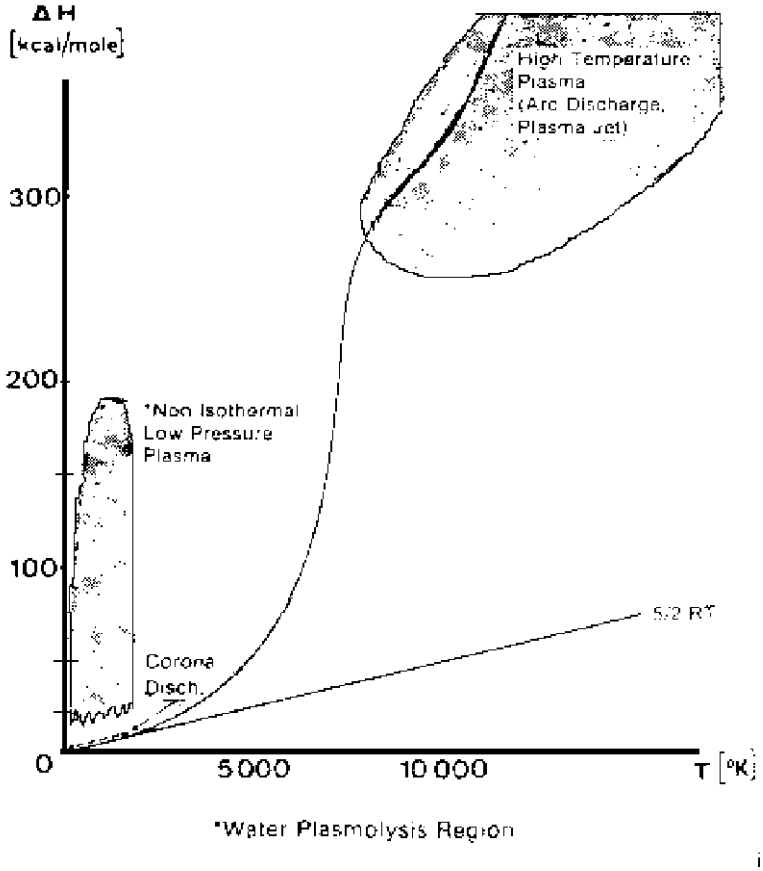

Figure 11
Glow Discharge Region Between Feed Ring and Nozzle

A high voltage DC electric power supply (PS-1) was used in some of the experiments to create a water-vapor glow-discharge between the water vapor feed-ring and the entrance to the ceramic dissociator-nozzle to enhance dissociation. See Figure 12. The applied voltage was measured with volt-meter V and the current with ammeter A.

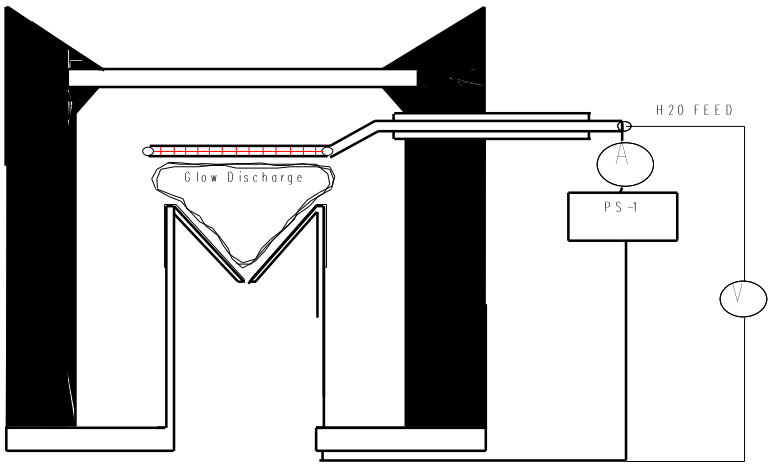

Figure 12
Glow Discharge Power Supply for Feed Ring and Dissociator-Nozzle

The partially dissociated water vapor was allowed to pass through the dissociator-nozzle throat and expand into a lower pressure region to form the jet and shock-wave. See Figure 13.

Higher Pressure Region

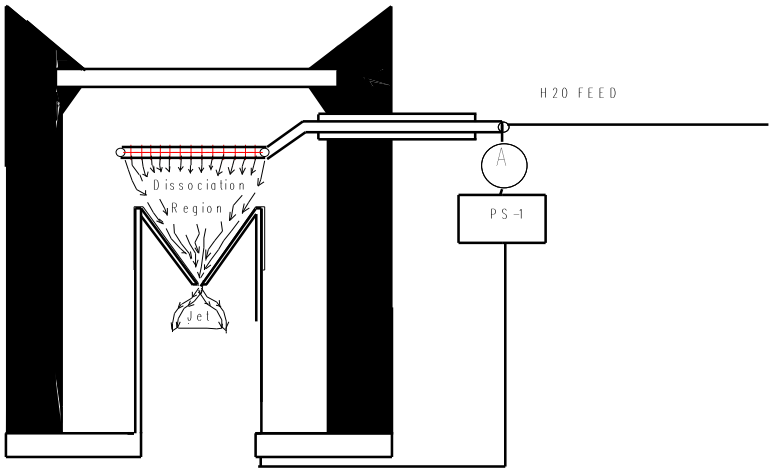

Lower Pressure Region

Figure 13
Water Vapor Dissociation and Expansion via Dissociator-Nozzle into Lower Pressure Region

The pressure ratio across the dissociator-nozzle was set higher than the critical ratio so that the gas velocity was sonic at the nozzle throat. The expanded gas flow down-stream of the nozzle throat reached supersonic velocity and a shock wave was formed in the lower pressure region at the nozzle exhaust. The gas mixture was cooled by the expansion from the nozzle, briefly re-

heated while passing through the shock-wave discontinuity, and further cooled downstream in the sub-sonic region while merging with the background gas.

Mass flow rate of water vapor to the reactor was measured as a function of pressure at the nozzle entrance and exit, and at the skimmer exit. See Figure 14.

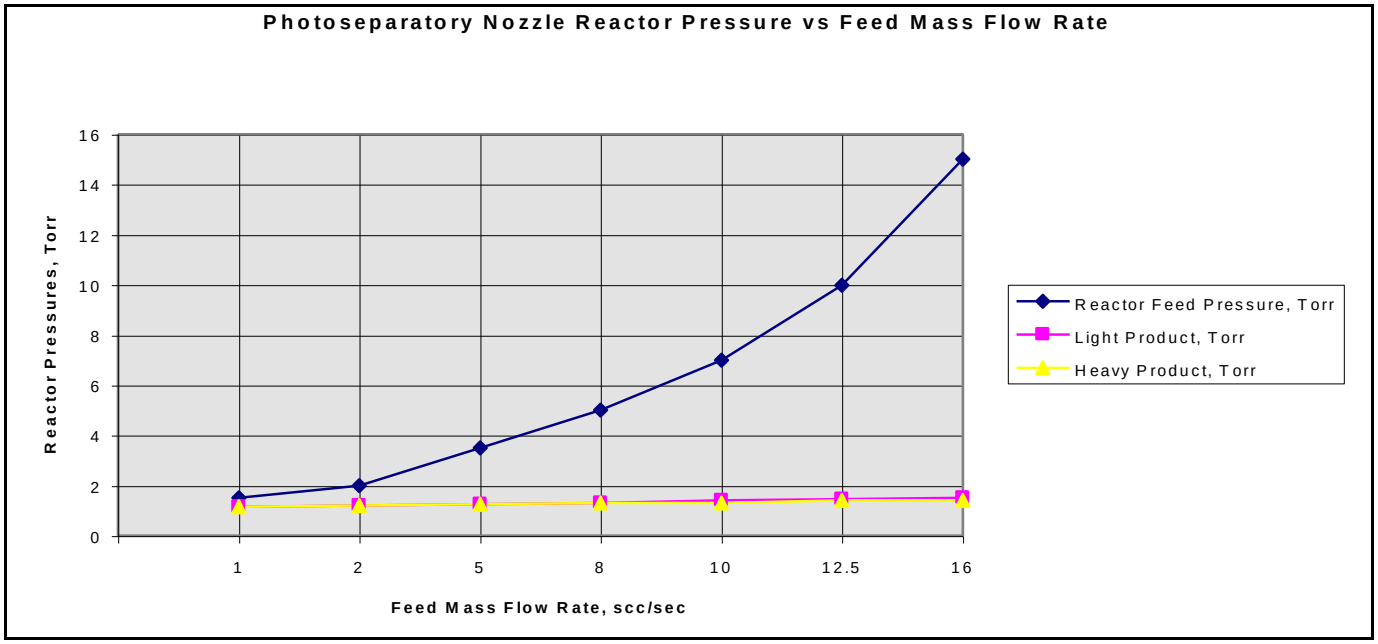

Figure 14
Reactor Pressures as a Function of Feed Water Mass Flow Rate

A supersonic beam skimmer was installed behind the shock wave to separate hydrogen and oxygen from the partially dissociated water vapor. See Figure 15. The circle shown in Figure 15, between the feed ring and the dissociator-nozzle, is where the solar image "fireball" and the water vapor glow-discharge region are located. The “fireball” is a three dimensional image of the sun that appears at the focal point of the concentrated beam. When viewed by an observer the solar image appears spherical (in free air with dust particles), regardless of the relative position of the observer, as with a hologram.

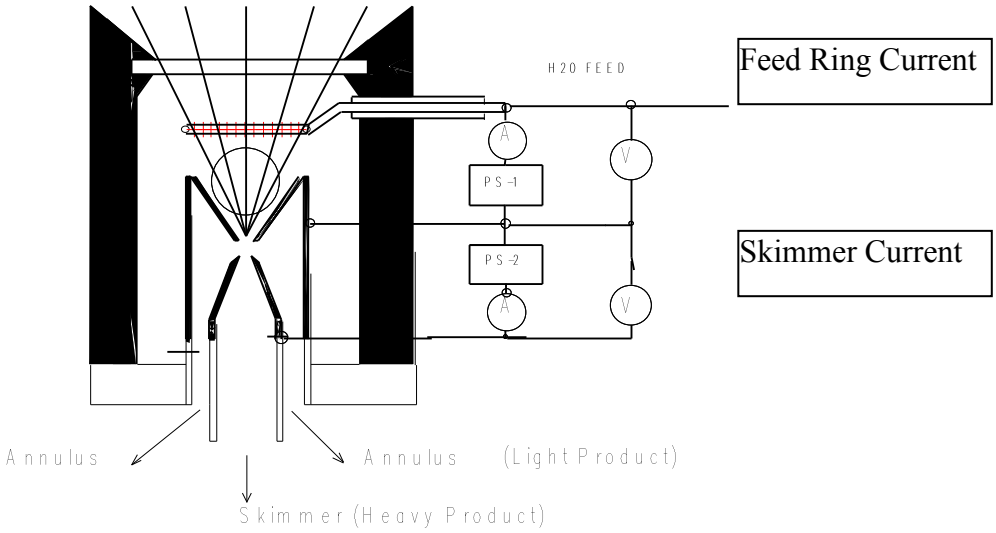

Figure 15
Skimmer Conical Nozzle Downstream from Sonic Dissociator-Nozzle

The supersonic beam skimmer used was a knife-edged cone. The skimmer was positioned with micrometers so that its entrance was at the down-stream edge of the shock-wave envelope. An appropriate pressure ratio was applied between the low pressure region and the beam skimmer to improve the separation factor for hydrogen and oxygen production. This jet separator functions by transverse gas diffusion. The hydrogen and oxygen (plus unconverted water vapor) are separated because the hydrogen gas diffuses transversely (relative to the jet flow axis, more rapidly than oxygen or water), due to its lower mass [55].

A second high voltage DC electric power supply (PS-2) was used to create a glow discharge between the sonic dissociator-nozzle and the conical skimmer nozzle to study separation enhancement by cataphoresis [88]. Cataphoresis is the spatial gas density gradient which forms near a cathode within a glow discharge. The minor gas component of a multi-component gas mixture will be enhanced at the cathode region of the discharge. Cataphoretic segregation in the positive column improves with increasing pressure (up to 40 torr) and increasing discharge current (up to 20ma) , and with decreasing initial concentration of the minority component. Cataphoretic efficiency has been observed to decrease with increasing temperature [88], however.

The glow-discharge between the dissociator-nozzle and the skimmer-nozzle also allows shock-wave visualization by a video camera which is aimed through a viewing slit in the reactor wall (Figure 5). The video camera is attached to a coherent optical fiber bundle and illuminated with a He-Ne laser through another incoherent optical fiber bundle to allow observation of the dissociator-nozzle and skimmer separation distance, as the skimmer is moved in or out of the jet.

Nozzle/Skimmer (Jet Separator) Theory

Development of nozzles and skimmers for gas separations can be traced back to separatory wall units studied in the early 1930's [54]. Extensive theoretical and experimental work on the application of supersonic jets and the separation-nozzle to gaseous isotope separations, molecular beam sampling systems, gas dynamic lasers, and combustion research was conducted from the 1950's until the present [55-81].

Nozzle Types

Supersonic nozzles have four general types of geometry:

- Laval
- Thin plate orifice
- Sonic
- Conical

See Figure 16. The geometry for a sonic or conic nozzle will be a round hole. Whereas for a Laval or thin plate orifice the hole can be round or a linear slot (channel flow). All of the nozzles in Figure 16 are shown with a round hole.

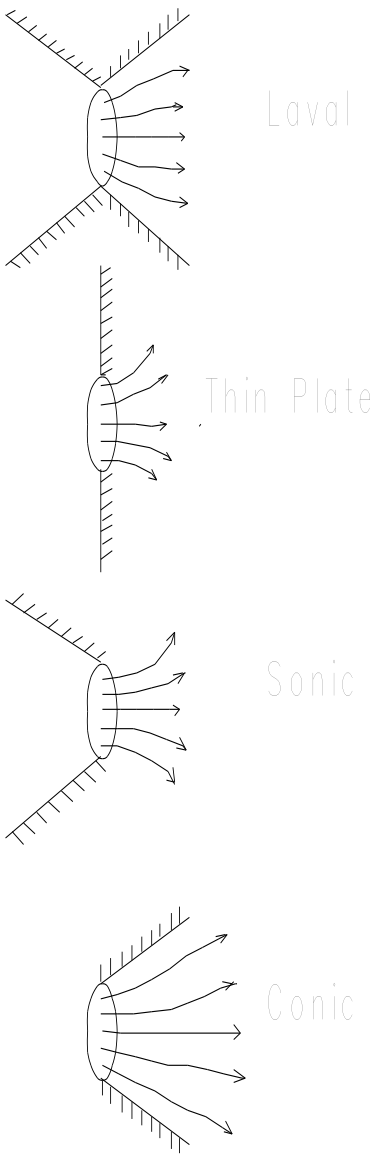

Figure 16
Supersonic Nozzle Exit Geometry's

In our application, which we call the Photo-separatory Nozzle reactor [32], sonic and conical geometry are used as shown in Figure 17 below [81]. In Figure 17 the sonic nozzle is on the left. We chose these sonic and conic shapes because they were the easiest to fabricate from quartz tubing in the laboratory.

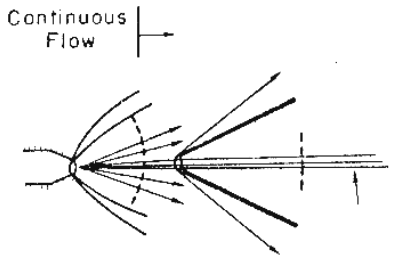

Figure 17
Photo-separatory Nozzle Reactor using sonic and conic nozzles

Nozzle expansion plume flow streamlines for sonic and Laval conical jet nozzles with "choked" flow (Mach number = 1 at the throat) are shown in Figure 18 below [81].

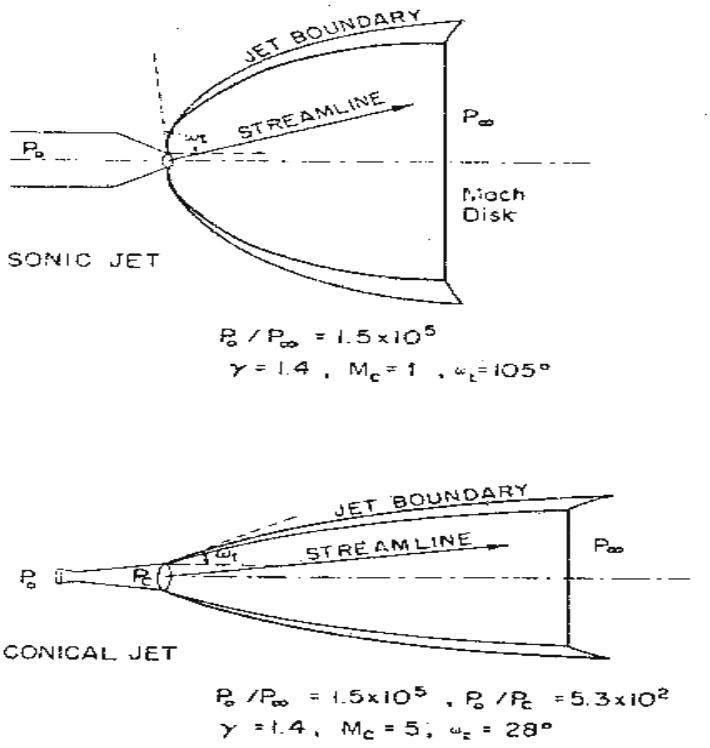

Figure 18
Sonic and Conic Nozzle Flow Streamlines and Shock Waves

Skimmer Theory

Skimmer conical nozzle flow streamlines are shown in Figure 19.

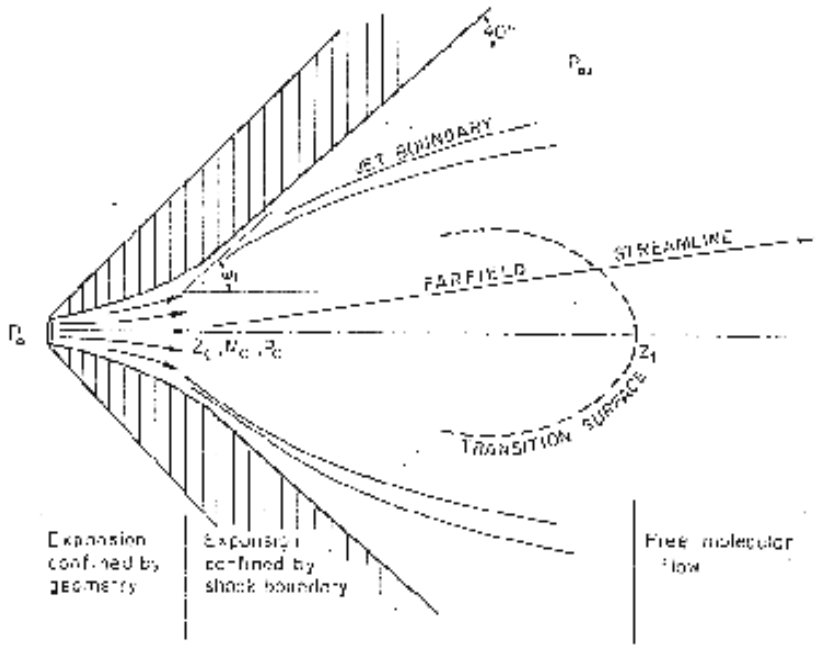

Figure 19
Skimmer Conical Nozzle Flow Cross Section

The cross section of the skimmer conical nozzle is shown in Figure 19 shows point Zc given as an apparent source for subsequent expansion in the inertia-dominated region. Before point Zc, flow is confined by the nozzle wall and after Zc, flow is confined by the shock boundary. The dashed line represents the transition surface between the continuous and molecular flow [81].

Enrichment of heavier-mass species occurs in the core of the gas jet. Enrichment of the lighter-mass species occurs in the periphery of the gas jet. The lighter and heavier species for a Photo-separatory Nozzle are depicted as a function of distance along the flow axis in Figure 20. The distance downstream of the nozzle throat, in millimeters, is shown as the ordinate (from bottom to top) in Figure 20.

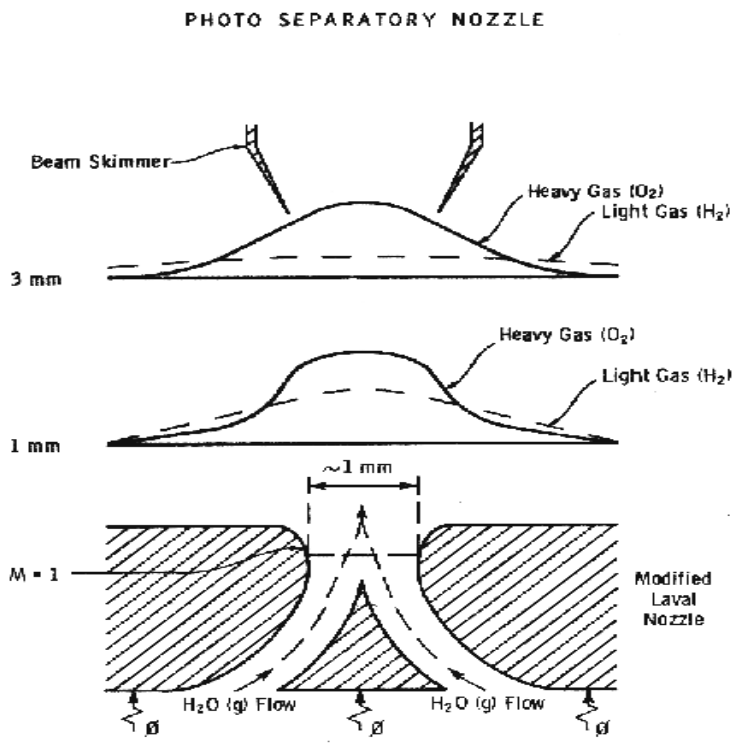

Figure 20
Photo-separatory Nozzle/Skimmer and Separation Factor
(Nozzle throat at bottom. Separated product moves toward the top.)

The free molecular diffusion separation arises from the disparity in the thermal velocity of light and heavy gas molecules, for gases with the same mass flow velocity and local temperature. The heavier species have a lower thermal velocity and expand less (laterally) after the transition plane, remaining more concentrated at the beam center [81].

Separation Factor =

[(Heavy Core Gas, M%) (Light Peripheral Gas, M%)]

[(Heavy Peripheral Gas, M%) (Light Core Gas, M%)]

Measurements were made with mixtures of 1% nitrogen in hydrogen and 1% argon in hydrogen to determine the separation factor obtained in a separatory-nozzle as the skimmer was moved in and out and laterally. See Figure 22 [81]. There is a region where alpha is a constant and linearly proportional to the mass ratio. This is a result of the "Mach number focusing" effect after the gas passes the skimmer orifice (due to the reflected wave off the skimmer's frontal surface.) The decrease in alpha as the skimmer is moved further downstream is interpreted as background gas pressure (down-field) penetration [81].

The combined effects of skimmer interference, a larger Mach number, and a minor species, give a decreasing value of enhancement factor n, when moving the skimmer close to the nozzle. In

moving the skimmer transversely a qualitative measurement of the degree of beam spreading is obtained.

The transverse profile of alpha versus skimmer position is given in Figure 22, which shows a much broader spreading for light species (hydrogen in this example) than for heavy species (argon in this example.)

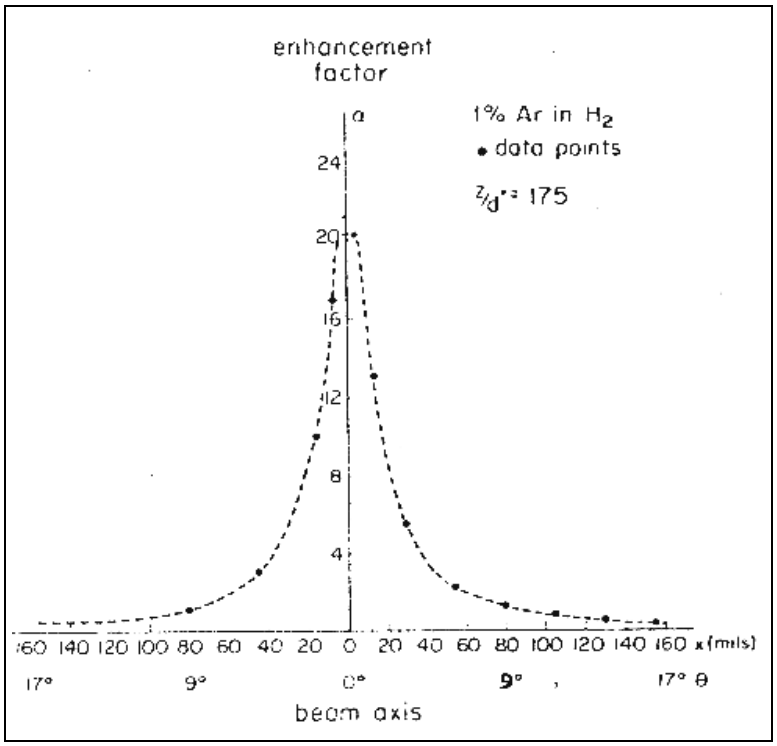

Figure 22
Traverse of Skimmer Across Sonic Nozzle Jet
Separation Factors Obtained with Ar/H2 Gas Mixture

In the case of a fixed skimmer-orifice dimension, an axially movable skimmer is necessary to achieve comparable beam intensities for different gases. The mass separation factor is approximately proportional to the mass ratio when the skimmer-interference and background-penetration effects are minimized [81].

Glow Discharge Theory

All gases at room temperature are excellent electrical insulators. In order to make them electrically conducting, a sufficient number of charge carriers have to be generated. Although there are normally a certain number of charge carriers present, the number is far too small to produce a measurable electrical conductivity. This small number of carriers present is the result of natural ionization of the gas by cosmic rays and radioactive substances [82-83]. If a sufficiently high electrical field is applied to a pair of electrodes separated by a volume of the gas, an electrical breakdown of the originally non-conducting gas establishes a conducting path through the electrode gap, producing an array of phenomena known as gaseous discharges[84].

In ascending order of current we find: non-self-sustaining discharges, Townsend discharges (self-sustaining dark discharges), normal glow-discharges, abnormal glow-discharges, and arc discharges. We desire a steady-state dc glow discharge for our solar plasma reactor, to obtain a higher electron population density.

In such a gaseous discharge a more or less electrically conducting plasma is generated which consists of a mixture of ions, electrons, and neutral particles. The composition and distribution of the plasma between the electrodes is a function of the existing discharge mode and other discharge parameters [84]. Our interest is in the glow discharge mode since a glow discharge can be made to function with relatively low electrical power consumption.

A glow discharge can be produced by the circuit shown in Figure 24 [85]. Resistor R is a current suppression (or ballast) resistor which limits the current through the gas-plasma after breakdown occurs. We used 10,000 to 18,000 ohm suppression resistors in the Photo-separatory Nozzle reactor.

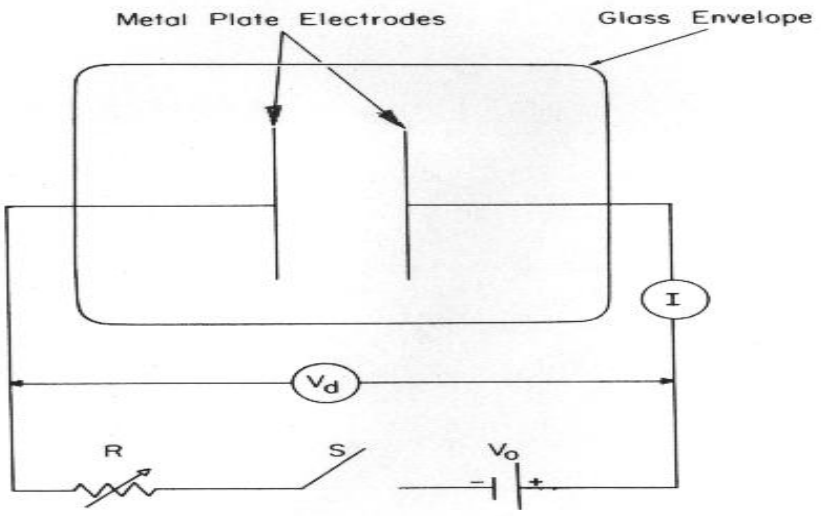

Figure 24
Glow Discharge Circuit

The time evolution of current I and discharge voltage Vd after switch S is closed will create a glow discharge in the reactor, provided that the power supply voltage Vo is greater than the breakdown voltage of the discharge tube [86].

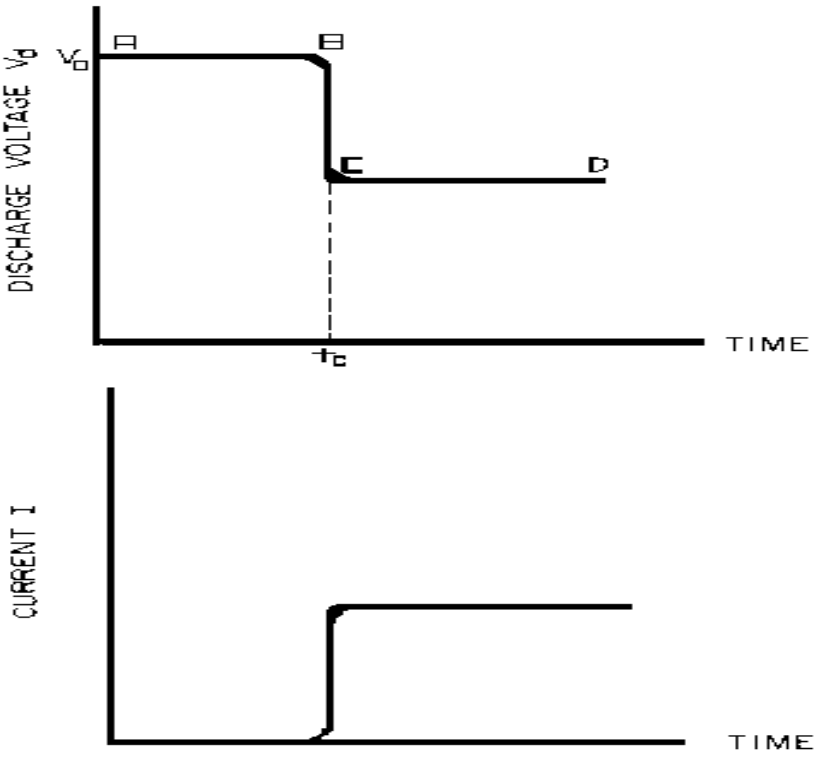

Figure 25
Time Evolution of Voltage and Current in A Glow Discharge After Switch S is Closed

For a length of time tc after switch S is closed, I is negligibly small and Vd is equal to Vo. After breakdown, which occurs for practical purposes at t = tc, the current rises and voltage drops to steady-state values, which are determined by the equation:

$$Vd = Vo - IR.$$

The discharge voltage Vd depends on **I** and certain properties of the discharge tube, such as gas type, gas pressure, electrode material, and electrode temperature. One part of the curve Vd versus time is called the dark discharge region. In this region there is little or no light detected by the human eye. The light intensity grows very rapidly after time tc reached, and a steady glow from the discharge, which may occupy most of the discharge tube, is observed thereafter. This part of the discharge is called the positive column and has a uniform light intensity. There are regions near each electrode, however, where the light intensity is not uniform [87].

At the negative electrode, called the cathode, there may be several light and dark layers, depending on the gas pressure and current. The cathode region has three main parts: cathode dark space, negative glow, and Faraday dark space. At the positive electrode, called the anode, there may be a region of light intensity brighter than the positive column, called the anode glow, and there is usually a dark layer, called the anode dark space, between these regions [87] .

At the cathode, most of the current is carried by ions flowing to the cathode. In the rest of the discharge, including the negative glow and the Faraday dark space, nearly all of the current is carried by electrons. The electrical characteristics of a glow discharge in a short tube without a positive column, such as we have in the Photo-separatory Nozzle reactor, can be divided into three main regions, that we can refer to as I, II, and III [87].

In region I extremely low currents, in the order of micro-amperes and less, produce a Townsend discharge with little or no visible light emanating from the tube. Region II can be subdivided into the normal glow region (low current) and the abnormal glow region (high current); this is a cathode related distinction. When the current is allowed to increase even further, the cathode fall undergoes a transformation from a cold-cathode discharge (high cathode fall) depending primarily on Townsend's first and second ionization processes, to a hot cathode discharge (low cathode fall) in which thermionic emission plays an important role [87,89]. The cathode fall is the electric field gradient through the cathode dark space.

For the Photo-separatory Nozzle reactor, heat is supplied to the dissociator-nozzle (which is also the cathode electrode for the glow discharge) by the concentrated solar beam, and it operates in region III[glow discharge with low cathode fall]. Cooling of the nozzle surface by electron boil-off occurs under direct thermionic emission process conditions at very high temperatures. Indirect emission processes (secondary emission processes) are also important to consider: electrons are ejected from the surface of the nozzle by energetic particles such as ions and photons in the glow discharge.

Ionization of Water Vapor.

Ionization of water vapor may occur by excitation of the molecule with electrons, to cause vibrational transitions. Vertical transition processes in polyatomic molecules which have been investigated include photo-absorption and photo-ionization [90]. The total absorption of electrons can result in ionization of $1b_1$, $2a_1$, $1b_2$, $1a_1$ electrons from the valence shell of water vapor [91].

The total inelastic dissociative attachment cross-section for water vapor is shown in Figure 28. When the low energy electrons are passed through water vapor two types of inelastic collisions occur (a) electronic excitation of the neutral molecules and (b) electron attachment to the neutral molecules. By summing the cross-sections for the production of OH^-, O^-, and H^- ions we obtain the total cross-section as a function of energy in electron volts [92]. These cross sections for attachment reactions were measured by carrying out the reactions in the ion source of a research mass spectrometer, with essentially constant detection sensitivity.

Ions from the negative glow and Faraday dark space of water vapor discharges are of the form $H_3O^+ \cdot (H_2O)_n$ where n = 0 to 5. The bond strength of the hydration reaction products decreases as successive water molecules add to H_3O^+, falling sharply beyond n = 3.[93] In the Photo-separatory Nozzle reactor the distance from the dissociator-nozzle (cathode) to the feed-ring is about 1 cm, so these important species are expected.[8]

Glow Discharge Applications to Hydrogen Production from Dissociated Water Vapor

In the Photo-separatory Nozzle reactor, the normal glow discharge voltage is interpreted as the minimum power supply voltage required to ensure that the electron energy is greater than the ionization potential, otherwise the glow would extinguish. In the dark (no concentrated sunlight), with water vapor pressures in the Photo-separatory Nozzle reactor's normal pressure regime, the power supply voltage required for sustaining normal glow may be about 700, whereas under concentrated sun-beam illumination the normal glow voltage is only about 200. The current requirement is on the order of 1-3 ma under either dark or illuminated conditions. The use of higher pressure required the use of higher current. The glow-discharge power is only a small fraction of the power arriving via the concentrated sun-beam, about 1 to 2 watts typically. This small electrical power requirement can easily be met by a photovoltaic cell array.

One of our early dissociator-nozzle designs used a quartz-to-metal electrical feed-through from the inside of the quartz tube to the outside zircon coating to provide cathode potential for the glow discharge in the "fireball" dissociation region. Zirconium-silicon oxide is formed from zirconia on quartz during “break-in” on-sun operation of a newly prepared dissociation-nozzle.

With this design, which we referred to as the "pilot" dissociator-nozzle, the glow-discharge was easier to ignite. This was due in part to the projection of the metal conductor (molybdenum) feed-through on the quartz dissociator-nozzle causing a field emission site, and in part to the closer proximity of the feed-through to the feed-ring (anode). According to Paschen's law the glow-discharge ignition potential is a function of the product of gas pressure and gap length only [89]. This design was abandoned due to problems with de-vitrification cracking and gas leakage at the electrical feed-through.

The present design of the dissociator-nozzle provides the cathode potential to the zircon coating via a platinum coating on the outside of the quartz dissociator-nozzle tube. This arrangement has been quite stable under many on-sun test runs, although the glow-discharge ignition procedure is different. With the present design we first ignite the dissociator-nozzle-to-skimmer gas space and obtain a glow-discharge, then we ignite the feed-ring to dissociator-nozzle gas space. Once the dissociator-nozzle-to-skimmer space has a glow discharge there is sufficient electron density to easily ignite the feed-ring to dissociator-nozzle gas space. The glow-discharge power for the lower pressure gas region between the dissociator-nozzle and the skimmer is of the same order as for the feed-ring to dissociator-nozzle power, 1 to 2 watts.

Description of Experimental Apparatus

The complete Photo-separatory Nozzle reactor assembly is shown in Figure 30. The reactor is mounted on top of a stage so that the concentrator mirror solar "fireball" image is focused inside the reactor, behind the window, on the dissociator-nozzle surface. Instrumentation for measuring pressures and temperatures, as well as the skimmer separator adjustment mechanisms can be seen.

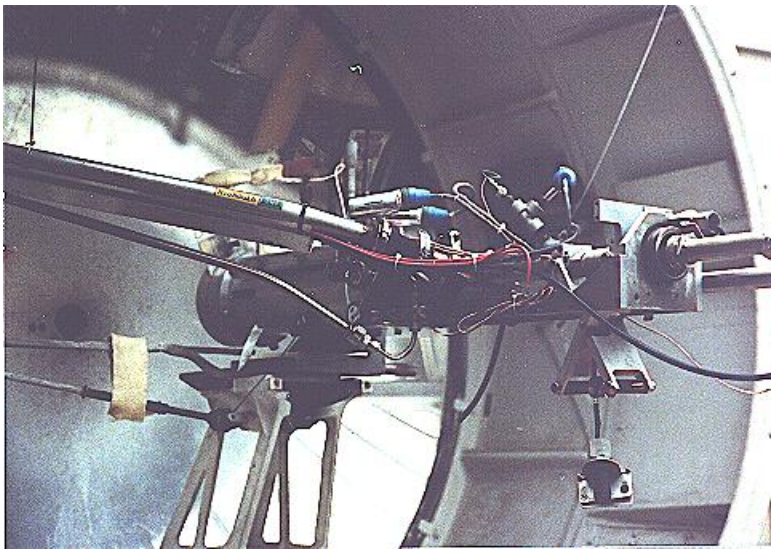

Figure 30

Photo-separatory Nozzle Reactor

Solar Beam Concentration System

Sun-light was concentrated by an elevation-azimuth two-axis tracking hyperbolic mirror. The 1.52 m (60 inch) mirror and its positioning gears came from a searchlight. The mirror is made of copper and plated with rhodium. The mirror is positioned by two stepper motors with self-contained stepper motor drivers. The stepper motor drivers were made by Electronic Products Co. , Model MD-1 and use the CY545 high performance stepper system control chip. The MD-1 interfaces to the computer via RS-232E lines connected to Communications ports 3 and 4. The overall gear reduction ratio was 400,145:1 for solar elevation tracking, so about 50,000 revolutions of the input motor were required to move the mirror +/- 23.5 degrees. This is about 10 million steps (200 steps/revolution) on the stepper motor.

Tracking accuracy must be maintained within 0.25 degrees to keep the concentrated beam "fireball" in the center of the dissociator-nozzle. An elevation angle sensor made by Schaevitz Sensing Systems Inc. was used to obtain mirror elevation information (Accustar electronic clinometer, ratiometric, vertical). For mirror azimuth position, a ten turn 10k ohm potentiometer was used with a reference voltage power supply across the pot. The pot was coupled to the base of the searchlight with a belt and pulleys so that the voltage from the pot slider changed as the azimuth changed. In the future we would like to use a fluxgate sensor to measure the azimuth position (KVH Industries Model MC 201 fluxgate compass, Middletown, Rhode Island).

A computer program written by H-Ion Solar, called Iontrack, calculates the elevation and azimuth of the sun based on the time of day, and the latitude and longitude of the mirror on the planet's surface. Iontrack reads the actual elevation and azimuth positions of the mirror from the two analog sensors, and determines the movement required for each axis to reduce the error to zero. Iontrack directs the two stepper motors to make the necessary movements to keep the tracking error under 0.10 degrees. As a practical matter the accuracy is limited by the accuracy of the elevation and azimuth sensors (about +/- 0.10 degrees).

Photo-separatory Nozzle Reactor Construction

The Photo-separatory Nozzle reactor was constructed from concentric nested quartz tubes and surrounded by a convection and conduction barrier (quartz double-wall evacuated and silvered) with radiant energy reflecting properties.

See Figure 31. An aluminum housing protects the quartz tubes, aligns and holds the silicone "O" ring seals in place, and serves as a mounting fixture on the stage of the searchlight concentrator. An optical viewing slit in the reactor containment vessel was provided for studying the transonic flow region, between the dissociator-nozzle and the skimmer.

Figure 31
Reactor Containment Vessel

Solar Beam Entrance Window

A quartz window admits the concentrated solar beam to the interior of the reactor. Inside the reactor, the gas feed-ring/electrode is positioned so that the converging solar beam passes through the feed-ring and the solar image "fireball" lands in the center of the trumpet-shaped dissociator-nozzle. See Figure 32. It is important to operate the reactor on-sun with water vapor flowing to the feed ring. In one experiment water vapor feed was interrupted and the stainless steel feed-ring was evaporated. The feed-ring turns black after operation on-sun for a few hours, but is not damaged by the beam as long as the water vapor feed is continuous.

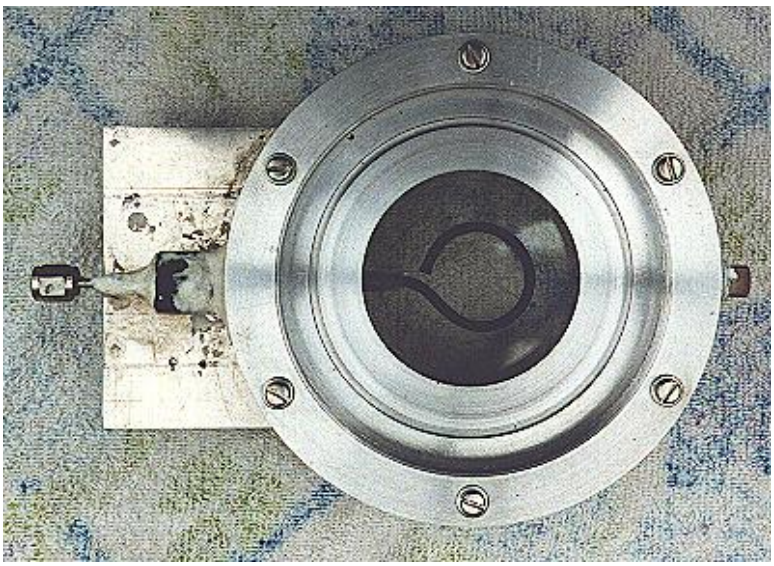

Figure 32
Solar Beam Entrance Window with Feed-Ring
(The inside diameter of the Feed-Ring is 2.78 cm)

An earlier reactor design introduced water vapor through the annulus between the reactors outer case and the dissociator-nozzle, and provided ionization of the water vapor by a needle-electrode. The needle-electrode was inserted through a hole drilled at the center of the solar-beam entrance window, and cemented in place. Although a glow-discharge could easily be established between the needle-electrode and the dissociator-nozzle, the needle tip was excessively heated by the solar-beam. The heating caused evaporation of the tungsten needle-electrode and subsequent undesired deposition of tungsten metal on the entrance window. As a result, we abandoned this design and adopted the feed-ring.

Sonic Dissociator-Nozzle/Electrode Fabrication

The dissociator-nozzle is a sonic nozzle with a trumpet-shaped converging entrance section made from a cylindrical quartz tube. A sealing flat flange was fused to the opposite end of the tube. A conductive thin film of platinum was applied to the outside of the quartz cylinder to provide an electrical connection (negative ground) for the dissociator-nozzle. The quartz tubing (General Electric Type 204 clear fused quartz) was coated with an yttria and calcia stabilized zirconium oxide refractory (Aremco Products Inc. Ultratemp 516 high temperature ceramic adhesive, Osining, New York) for the reaction zone and solar beam target.

The sonic quartz dissociator-nozzle is shown in Figure 33.

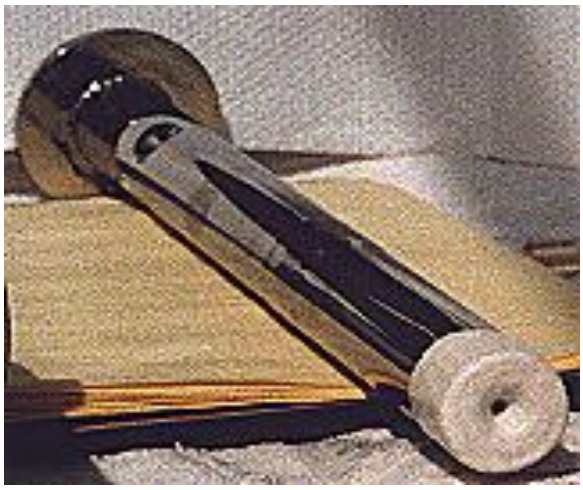

Figure 33
Sonic Quartz Dissociator-Nozzle with Ceramic Zirconia Coating

A special process was developed for application of the ceramic coating on the nozzle. By following a time-temperature ramp program we were able to prevent bubbles from forming due to violent off-gassing during firing, and provide a smooth surface coating of zirconia ceramic on the quartz substrate.

After 10 to 20 hours of on-sun operation, samples of a broken zirconia-on-quartz dissociator-nozzle were analyzed by x-ray diffraction. Zircon (zirconium-silicon oxide) micro crystals were detected, indicating a new conductive interface layer had been formed between the quartz tube and zirconia coating. Better thermal-expansion matching of materials seems to be obtained with a zircon layer. De-vitrification cracking of the quartz substrate and crumbling of the zirconia coating are no longer problematic. A glassy surface finish is produced on the heat-affected portion of the dissociator-nozzle coating after “break-in”.

Gas (Water Vapor) Feed-Ring Electrode

The feed-ring electrode was made from a loop of stainless steel tubing. The tubing was welded closed at one end and drilled with feed holes 0.508 mm(0.020 inches) diameter chamfered 1 mm (0.040 inches) periodically at 1.27 cm (0.5 inch) intervals along its length. The tubing was then rolled around a mandrel to form the feed-ring electrode. A quartz tubing sleeve was used as a feed-through insulator at the reactor window retainer wall to supply reactant gas and electrical power. The electrical power supply connection to the feed-ring electrode is made outside the reactor on the stainless steel gas feed tube. See Figure 34.

Figure 34
Gas (water vapor) Feed-Ring Electrode
Inside diameter of Feed-Ring is 2.78 cm(1.094 inches). Tubing outside diameter 0.318 cm (0.125 inches).

Skimmer Nozzle/Electrode

The skimmer nozzle/electrode is a conical nozzle that is mounted on the end of a cylindrical stainless steel tube which fits coaxially inside the cylindrical dissociator-nozzle tube coaxially. The conical skimmer-nozzle/electrode entrance faces the dissociator-nozzle's exhaust jet. The conical skimmer-nozzle was fabricated from a sharp-edge truncated cone made of quartz tubing and ground to a knife-edge using a diamond abrasive wheel. The quartz skimmer-nozzle was coated with platinum for electrical conductivity and connected (via a feed-through) to an electrical power supply on the outside of the reactor. See Figure 35.

Skimmer nozzle sharp edge orifice is 1 mm in diameter.

Skimmer quartz tube

Inside diameter = 12.8mm.
Outside diameter = 14.8mm.
Overall Length = 5.5cm

Maria

Outside diameter = 17mm.
Width = 3mm.
Length = 2.5cm (to the right of Maria)

Figure 35
Conical Skimmer Nozzle/Electrode

Product Separation Control System

A scissors jack is used to move the skimmer in and out with respect to the dissociator-nozzle exhaust axis. The scissors jack counteracts the forces on the skimmer caused by atmospheric pressure exerted on one side of the skimmer and the lower process pressure on the inside of the skimmer. An electronic proximity sensor and a dial gauge are used to provide axial position information. The spacing between the dissociator-nozzle and skimmer is of the order of one nozzle diameter (about 1mm.) The skimmer can be moved from about 0.1mm to about 2.0mm downstream of the dissociator-nozzle. Depending on the pressure in the region between the dissociator-nozzle and the skimmer this distance is approximately 1 mean-free-path (between atom/molecular collisions).

An eccentric is used to move the skimmer from right/left and up/down around its pivot point. The pivot point is located about 22 cm downstream from the dissociator-nozzle's exit orifice. The pivot point is made from 3 dimples inside the dissociator-nozzle tube. Two more proximity detectors and dial gauges provide up/down and right /left skimmer position information.

Product Gas Sampling System

Sampling valves are located in the two product discharge lines. Each sampling valve can admit product gas into the mass spectrometer. The spectra from each product line are alternately taken; then the mass spectrometer background gas pressure spectrum is subtracted from each. Finally the mass ratios for the light and heavy products are calculated and used to obtain a separation factor. The mass spectrometer sampling system is shown in Figure 36.

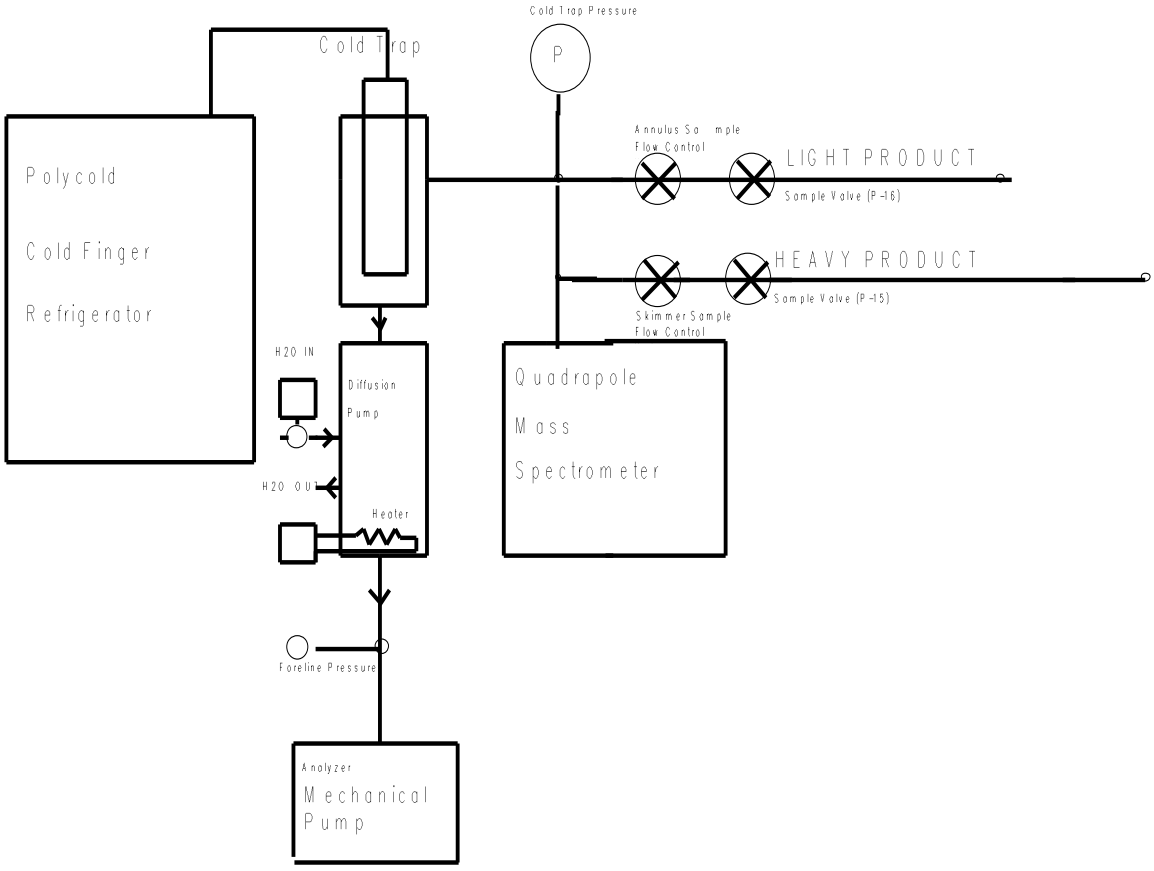

Figure 36

The quadrapole mass-spectrometer is a model QUAD 1210 residual gas analyzer made by CVC Products Inc. (Rochester New York). The Polycold refrigeration unit has three stages to cool the cold-trap (and cryo-pump water vapor.) The cold-trap also prevents diffusion pump oil from back-streaming into the analyzer. The diffusion pump is a Consolidated Electromagnetics Corp. model MCF 60-1. The mechanical pump is a Sargent-Welch model 1376. The sampling leak valves are Nupro model SS-4-BMG bellows needle valves. The sample admission valves are Nupro SS-4BK-1C miniature air-operated bellows valves with M-SOL-2K solenoid actuators for electrical control by computer.

Description of Data Acquisition Hardware and Software

The data acquisition system uses two Data Translation DT-2805 analog to digital (A/D) converter cards with an IBM compatible 386 computer. Each A/D card provides eight analog inputs. One card is used primarily for temperature and radiation information, and the other is used for pressure, mass spectrometer and mass flow rate inputs.

Analog Inputs to DT 2805

Board 1 (Address 2EC hex)

Channel 0 ....Thermocouple Reference Junction
Channel 1.....Feed Gas Temperature
Channel 2.....Light Product Temperature
Channel 3.....Heavy Product Temperature
Channel 4.....(Spare)
Channel 5.....Quartz Window Retainer Temperature
Channel 6.....Reactor Case Temperature
Channel 7.....Epply Radiometers (select any one of four)

Board 2 (Address 2F4 hex)

Channel 0.....Mass Spectrometer Trigger (Sweep)
Channel 1.....Mass Spectrometer Partial Pressures
Channel 2.....Feed Ring Pressure
Channel 3.....Light Product Pressure
Channel 4.....Feed Gas Mass Flow
Channel 5.....Light Product Mass Flow
Channel 6.....Heavy Product Skimmer Pressure
Channel 7.....Heavy Product Mass Flow

The data acquisition software used includes: Lab Tech Notebook V. 9.0 and a custom display program written by H-Ion Solar Co. called PSR23. PSR23 displays the analog data taken from the temperature, pressure, radiation, mass flow transducers (by Lab Tech Notebook) on the computer screen. PSR23 operates the mass spectrometer sampling valves, to sample the light and heavy product lines, and displays the most recent mass spectra on the computer screen. PSR23 is being modified to archive the sampled mass spectra in time and date stamped files, for analysis at the end of a run.

Pressure Transducers

Pressure transducers were installed upstream and downstream of the dissociator-nozzle to measure the pressures for use in calculating the pressure ratio and data logging of the feed pressure and expansion jet background pressure. Another pressure transducer was installed on the inside of the skimmer tube so the pressure ratio could be calculated and the data logged. The operating range of the Granville-Phillips Series 275 analog readout "Convectron" vacuum gages is

1 milliTorr to 1000 Torr. The analog meter face digitally displays the data, however, the analog output of each gauge must be linearized by a cubic-splines computer transform before data logging (done by H-Ion program PSR23).

Thermocouples

Type J thermocouples were used for temperature measurements. The thermocouples were linearized and scaled within the data acquisition program Lab Tech Notebook.

Mass Flowmeters

The mass-flow rates of the water vapor feed and the skimmer (heavy product) and annulus (light product) were measured with Teledyne Hastings-Raydist model ST and model HFM-200H mass flow meters. The mass-flow meters were powered, digitally displayed, and scaled for computer analog input by a Teledyne Hastings-Raydist model PR-4A four channel flow monitor.

Using the three mass-flow meters allowed us to perform a mass balance across the reactor to obtain measurement closure with the flow meters (as a calibration and leak check.)

Optical Pyrometer for Nozzle Surface Temperature Measurement

A Pyro Micro-Optical Pyrometer made by the Pyrometer Instrument Company Inc. (Northvale N.J.) was used to measure the temperature of the dissociator-nozzle surface under different operating conditions. The instrument includes a telescope, pyrometer lamp filament, power supply, and filament current meter. We used an EC-6 high temperature range filter and a 90 degree M-14 prism to view the dissociator-nozzle. Corrections to the indicated temperature were made for the prism, the filter, the range selection, and the reactor window transmission loss for any given temperature.

We normally measure temperatures in the 2300 K to 2800 K range at the nozzle surface, depending on the water vapor feed pressure and the solar beam flux. Stagnation temperatures as high as 3250 K have been measured on the nozzle surface (somewhat higher than the published melting point of zirconia.)

Pumping Requirements

Pumping the products from low pressure to atmospheric pressure or higher requires compression work, which is a parasitic loss in the overall efficiency of the process. The losses for the oxygen-rich stream compressor and the hydrogen-rich stream compressor must be minimized by selecting reactor pressures no lower than necessary, and by the use of efficient compressor designs.

Our reactor uses two Sargent Welch model 1397 rotary vane vacuum pumps to pump the skimmer and annulus. Two Bell model CG100A clamp-on AC ammeters and two Fluke model 8020A digital volt-meters are used to measure the work done (power in watts) by the two vacuum pumps. With no feed-water flow and thus no product flow through the two vacuum pumps, 1245 and 1233 watts respectively were required to maintain the process vacuum. When maximum flow of feed water vapor to the reactor was provided (82.9 sccm), the vacuum pumps required 1254

and 1242 watts respectively. The net power required to pump the process fluids is then 9 + 9 = 18 watts. It could be seen that the efficiency of these lab vacuum pumps is quite low.

Two types of compression can be considered: iso-thermal and adiabatic.

Iso-thermal Compression

For the iso-thermal case, compression reduces the volume of the gas and increases the pressure in a pressure-volume diagram, while undergoing perfect cooling, so that the gas remains at the inlet temperature while being compressed. This process requires less work than the adiabatic process. Isothermal compression work is expressed as:

$$W = R\,T\,\ln(P_2 / P_1)$$

Where R is the gas constant, T is the inlet temperature in deg. K and P1/P1 is the pressure ratio across the compressor in atmospheres. For 1 Torr to atmosphere at 300 K inlet temperature the work is about 16.7 kJ/g-mole (4 kcal/g-mole).

Adiabatic Compression

In the adiabatic case, compression reduces the volume and increases the pressure along a different path of the pressure-volume diagram with no cooling. It is not possible to provide isothermal conditions during our compression without multiple stages and intercoolers, therefore we use the adiabatic case for our estimates. Adiabatic pressure head H_{ad} across the vacuum compressor is defined as:

$$H_{ad} = [\gamma / (\gamma - 1)]\,R\,T[(P_2 / P_1)^{\{(\gamma-1)/\gamma\}} - 1]$$

Where R is the universal gas constant, γ is the ratio of specific heats (at constant volume and constant pressure) for the gas mixture, and T_1 is the absolute temperature in deg.K at the compressor inlet. The compression work W_c is expressed as:

$$W_c = \int_b^c P\,dV$$

Where the integral from b to c is the work required to proceed along a polytropic pressure-volume diagram curve from low pressure b to higher pressure c.

The adiabatic power $P_{ad} = [(m)\,(H_{ad})]/K$, where m is the mass flow rate, K is a unit conversion constant, and H_{ad} is the adiabatic pressure head.

To compress the products adiabatically (no cooling) from 1 Torr to one atmosphere with an inlet temperature of 300 K would require about 50 kJ/g-mole (11.9 kcal/g-mole). Isothermal compression (with intercooling) would require only about 1/3 as much compression work.

The final adiabatic compression temperature would be determined as $T_2 = T_1\{ (P_2/P_1)^{[(\gamma-1)/\gamma]}\}$.

For 1 Torr at 300 K to atmosphere compression we obtain 2000 K discharge temperature using this calculation. The actual temperature at our pump discharge is much lower than 2000 K, due to heat transfer to the pump and piping which provides distributed intercooling of the process gas.

Energy Balance:

An energy diagram which gives estimates for the losses in the process, both to the surroundings, and to parasitic power requirements is shown in Figure 37.

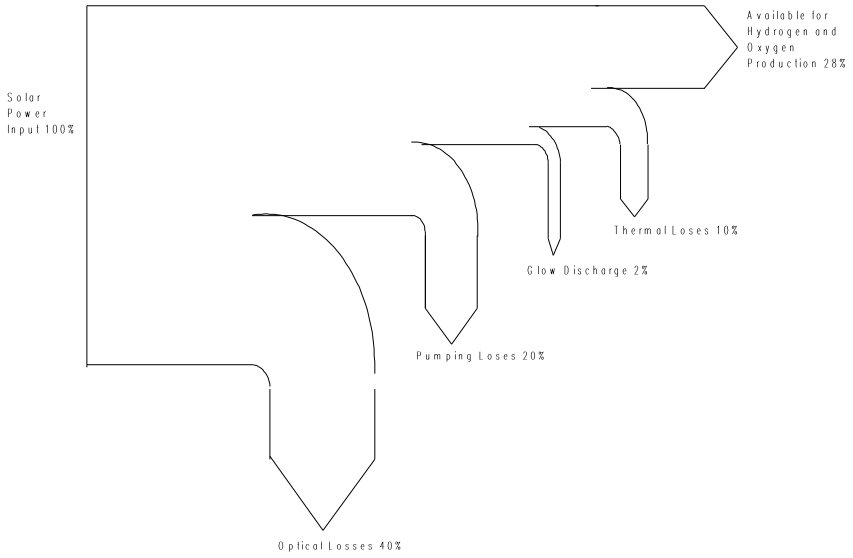

Figure 37

The optical losses can be reduced through:

1) Use of a higher quality solar concentrator mirror.

2) Use of a dome shaped solar-beam entrance window instead of a flat window.

3) A receiver geometry resembling a cavity.

The pumping losses and glow-discharge losses are in reality electrical power requirements, which, if met by photo-voltaic means, can be considered a capital cost.

Experimental Separation Efficiencies and Solar-to-Hydrogen Efficiencies to Date

Experimental solar-to-hydrogen efficiencies to date are shown in figure 38 below. The first bar on the (labeled DTH) is the direct thermal hydrogen conversion efficiency obtained by analyzing the dissociator-nozzle jet flow-field without the use of a glow discharge or skimmer. About 1.1% solar-to-hydrogen (higher heating value) conversion was obtained.

The second bar (labeled DTH Glow) shows an improvement in solar to hydrogen conversion to about 2.1% when a glow discharge was applied and the skimmer and annulus hydrogen production was added together. The maximum and minimum measured values are shown about the mean.

The third bar (labeled PVE1) shows the solar-to-hydrogen efficiency obtained using silicon photovoltaic cells and an alkaline electrolyzer [94]. The fourth bar (labeled PVE2) shows the results of another photovoltaic electrolysis system [95].

The conversion efficiency for a solar dish Stirling generator combined with an alkaline electrolyzer 75% efficient [96] is labeled SSE in Figure 38.

The next bar (labeled NREL Goal) shows the long term solar-to-hydrogen efficiency goal established by the National Renewable Energy Laboratory, for reference purposes.

Multi-junction single crystal gallium arsenide solar cells with future 37% solar-to-electrical efficiency combined with a 75% efficient alkaline electrolyzer [97] is labeled PVE Ga As.

The bar (labeled DTH Future) indicates that the future direct thermal hydrogen process may compete with other known methods on an efficiency basis. It may have the further advantage that it does not use expensive single crystal materials.

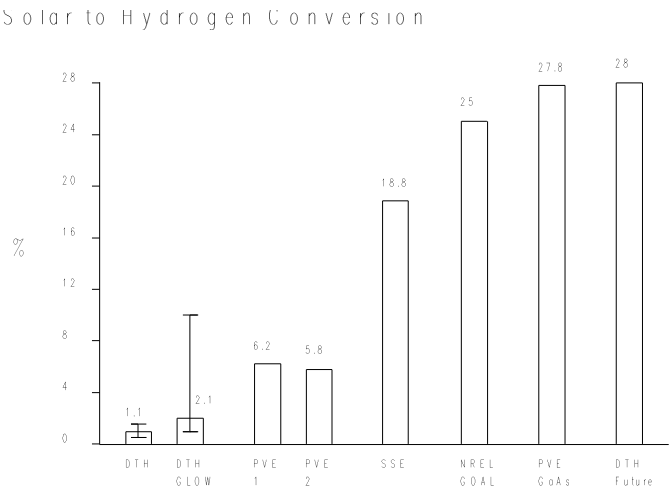

Figure 38

Theoretical Solar-to-Hydrogen Efficiencies Possible Based on Literature Review and Experimental Experience

The process efficiency, N_p, of a process that separates water dissociation products at low pressure and then compresses them to atmospheric pressure is [98]:

$$N_p = H / (Q + W_S + W_C)$$

Here H is the enthalpy of formation of liquid water, Q is the thermal energy input, W_S is the separation work, and W_C is the compression work. In Figure 39 the process efficiency is calculated for two pressures assuming 100% separation and compression efficiencies, so the actual efficiencies will be lower at every temperature.

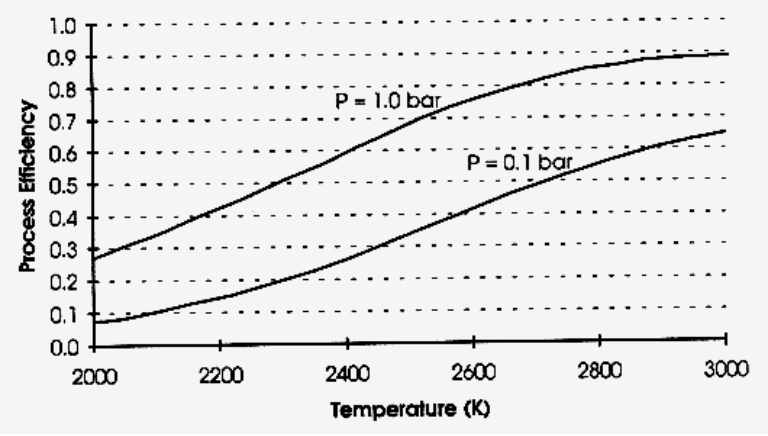

Figure 39
Process Efficiencies for Ideal Separation and Compression

The overall system efficiency is the product of the process efficiency and the solar collection efficiency. The result is plotted in Figure 40 for a system pressure of 1 bar. These calculations indicate that the process temperature should be around 2500 K [98].

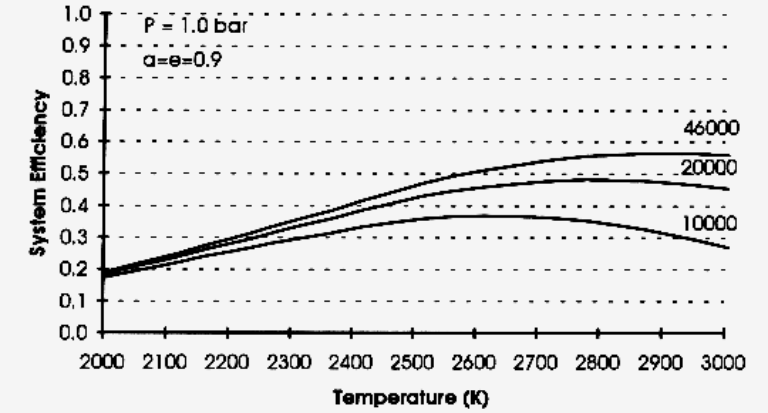

Figure 40

Recommendations for Future Research and Experimentation

We have seen that some direct thermal hydrogen production can be obtained in this reactor simply by passing water vapor through a hot ceramic nozzle (1.1%). We have also found that impressing a glow-discharge across the dissociator-nozzle almost doubles the conversion (2.1%). The separation factor for the skimmer has not yet been optimized. More work remains to obtain accurate spatial calibration of the skimmer, and investigate the effect of pressure, flow separation, and glow discharge on the separation efficiency. At this time the amount of recombination which occurs after dissociation is unknown. However, we feel there are very exciting possibilities for improvement of the process.

Further improvements in product gas analysis (mass spectrometer)calibration and skimmer nozzle position calibration are needed to remove uncertainty from the measurements and provide real-time data during on-sun experimental runs.

Statistical Experimental Design:

A statistical 1/2 factorial experimental design is proposed below to investigate the operating conditions attainable in the Photo-separatory Nozzle reactor.

Input Variables

- Solar Flux, kW/m^2
- Nozzle Temperature, deg. K
- Feed-water Mass Flow, sccm saturated vapor
- Feed-ring steam pressure, Torr (mm Hg)
- Glow Discharge on/off
- Skimmer Distance from Nozzle
- Hydrogen Annulus Pressure, Torr (mm Hg)
- Hydrogen Compressor Power, watts
- Oxygen Skimmer Core Pressure, Torr (mm Hg)
- Oxygen Compressor Power, watts

Total = 10 input variables.

Output Variables

- Oxygen Skimmer
  - ⇒ Hydrogen, mole %
  - ⇒ Oxygen, mole %
  - ⇒ Water, mole %
  - ⇒ Mass Flow Skimmer, sccm
- Hydrogen Annulus
  - ⇒ Hydrogen, mole %
  - ⇒ Oxygen, mole %
  - ⇒ Water, mole %
  - ⇒ Mass Flow annulus, sccm

Total = 8 output variables.

Sequential Tests

Sequential tests should proceed a factorial design to determine the practical limits for each of the ten input variables.

1/2 Factorial Design

Applying a 1/2 factorial statistical experimental design would require a minimum of two input levels for each input variable. For 10 input variables at two levels we would have $2^{10} = 1024$ tests. For 1/2 replicate we would need 2^{10-1} or 512 tests. It can be seen that reduction of the number of input variables by even one, has a large effect on the number of tests required for a 1/2 factorial experimental design. A sensitivity analysis can be done following the sequential tests to see if one or more variables can be omitted from this experimental design.

Mass Spectroscopy Software

Improvements to the mass spectroscopy software are needed to provide more accurate partial pressure measurements for speciation of the product gas streams; this will allow us to better determine the separation or enhancement factor between the hydrogen-rich product stream and the oxygen-rich product stream.

Water Tolerant Vacuum Compressors

Improved vacuum compressors that are tolerant to water are needed to improve the reliability of the system, or an easy means of trapping-out unconverted water-vapor prior to the pumps is needed. Vacuum pumps which gave problems had micarta rotary vanes. The micarta vanes expanded when exposed to water vapor and became too tight in the rotor to be returned by their springs. By replacing the micarta vanes with steel vanes and lowering the pump speed, good water tolerance and longer pump life are expected. More efficient vacuum compressors will be needed for a practical unit in the scaled up form.

Plasma Discharge Optimization

Radio frequency power supplies have been applied alone, and super-imposed on the d.c. for plasma discharges in the dissociator region and the skimmer orifice region. More work needs to be done to match the impedance of the radio frequency power supply to the reactor, and allow wider frequency spectrum capabilities. Radio frequency wave-form synthesis (modulation) can also be used to influence the nuclear magnetic resonance of the gas molecules (such as proton NMR). It would be interesting to attempt to duplicate plasma centrifuge effects reported by others [99] under our operating conditions in the solar reactor.

Micro-nozzle Arrays

Micro-nozzle arrays may allow possible scale-up of the process for a wide area solar reactor receiver with smaller mean-free-path dimensions and thus higher operating pressures and lowering of parasitic compression work on the products [100-105].

Scale-Up

Many small reactors or fewer large reactors can be used to obtain commercially attractive amounts of hydrogen and oxygen.

Scale-up strategies include:

1. Large dish-shaped mirrors or several smaller multi-faceted mirrors concentrating sunlight on a large planar array of small nozzles at the focal point.
2. A multiplicity of smaller mirrors and smaller targets with one or just a few small nozzles.

The arrays can be arranged in matrices or linearly. We can envision the arrays of solar-hydrogen reactors strung out along two parallel pipe lines, running from a remote desert area with high insolation, to supply cities. Existing natural gas pipelines could be used to transport the hydrogen and oxygen products separately to their point of use. Alternatively, one pipeline could be used to transport hydrogen to the point of use and the oxygen could be vented.

REFERENCES:

[1] J.J. O'Gallagher, R. Winston, A. Lewandoski, **The Development of Two Stage Non-imaging Concentrators for Solar Thermal Applications**, ASES Solar 93 Conference, Wash.D.C. April, 1993

[2] JANAF, **Thermochemical Tables**, U.S. Dept.Commerce, National Bureau of Standards, B.P., 168370, 1, (2) (1965-1969).

[3] P.R. Ryason, E. Hirsch, **"The Hydrogen Oxygen Reaction -I"** ,California Research Corp. Richmond, California , December 7, 1962.

[4] Hirsch, E., **"Concentration of Free Radicals During the Induction Period of the Hydrogen - Oxygen Reaction"**, Californa Research Corp., Richmond, California, May 17, 1963.

[5] Hirch, E. , **"Interupted Hydrogen Oxygen Reactions"**, California Research Corp. Richmond, Callifornia, May 1964.

[6] S. Gordon, B.J. McBride, **Computer Program for Calculation of Complex Chemical Equilibrium Compositions, Rocket Performance, Incident and Reflected Shocks, and Chapman-Jouguet Detonations**, NASA SP-273, NASA, Washington D.C., 1971

[7] E.A. Fletcher, **Technical Discussion: Comment on Feasibility of Hydrogen Production by Direct Water Splitting at High Temperatures**, Int.J. Hydrogen Energy Vol.4, pp.225-227, (1979).

[8] T.A. Melik-Asloanova, A.S. Abbasov, V.I. Shilnikov, **Dissociation of Water Vapor in Supersonic Flow of Non-equilibrium Plasma**, Inst. of Physics Azerbaijan, Baku, p.1063-1069, World Hydrogen Energy Conf. 2, 1978.

[9] V.P. Bochin, A.A. Fridman, V.A. Legasov, V.D. Rusanov, G.V. Sholin, **Hydrogen Production in Non-equilibrium Plasmachemical Systems**, I.V. Kurchatov Inst.of Atomic Energy, Proc. World Hydrogen Energy Conf. 2, Zurich, Vol.3, pp.1183-1208, 1978.

[10] I.G. Belousov, V.A. Lagasov, V.D. Rusanov, **Plasmochemical Cycle of Hydrogen Production from the Water**, Kurchatov Inst. Atomic Energy, World Hydrogen Conf. 2, 1978.

[11] A.Z. Bagautdinov, V.K. Jivotov, J.I. Eremenko, I.A. Kulachev, S.A. Musinov, A.M. Pampushka, V.D. Rusanov, **High Power Plasma Chemical MCW-Plant for Hydrogen Production**, Kurchatov Inst. Atomic Energy, World Hydrogen Energy Conf. 2, pp255-260, 1978.

[12] V.K. Givotov, A.A. Fridman, M.F. Krotov, E.G. Krasheninnikov, B.I. Patrushev, V.D Rusanov, G.V. Sholin, **Plasmochemical Methods of Hydrogen Production**, Kurchatov Inst. Atomic Energy, Int. J. Hydrogen Energy, Vol.6, No.5, pp.441-449, 1981.

[13] J.O'M. Bockris et al, **On the Splitting of Water**, Int Jour. Hydrogen Energy, Vol. 10 no. 30, pp. 179-201 1985.

[14] J. Lede, C. Weber, J. Villermaux, M.A. Brown, **Thermique.-Evaluation de l'efficacite d'un dispositif permettant de realiser des chocs thermiques sur des gaz par concentration d'energie solaire**, C.R. Acad.Sc.Paris,t.286(5 juin 1978)Serie B 299-302.

[15] J.Villermaux, J.Lede, **Chimie et Energie Solaire**, La Recherche No.149, Novembre 1983, Vol.14, p.1346-1357.

[16] J. Lede, F. Lapique, J. Villermaux, B. Cales, A. Ounalli, J.F. Baumard, A.M. Anthony, **Production of Hydrogen by Direct Thermal Decomposition of Water, Preliminary Investigation**, Int.Jour.Hydrogen Energy, Vol.7, No.12, pp.939-950, 1982.

[17] F.Lapique, J.Lede, J.Villermaux, B. Cales, J.F.Baumard, A.M. Anthony, G.Abdul-Aziz, D.Puechberty, M.Ledoux, **Recherches sur la production d'hydrogene par dissociation thermique directe de la vapeur d'eau**, Entropie No.110, 1983, pp.42-53.

[18] F.Lapicque, J.Lede, J.Villermaux, J.Robieux, **Cinetique Chimique.-Production de monoxyde de carbone par decomposition thermique directe de dioxyde de carbone**, C.R. Acad.Sc.Paris, t.298, Serie II, No.6, 1984, p.191-194.

[19] J.Lede, C.Braun, F.Lapique, J.Villermaux, B.Cales, Y.Nigara, A.M. Anthony, G.Abdul-Aziz, P.Puechberty, M.Ledoux, **Preparation d'hydrogene par thermolyse de l'eau,** Entropie No.116/117, 1984, p.15-25.

[20] F.Lapique, J.Lede, J.Villermaux, **Reacteurs de Trempe dans les Procedes Chimiques a Haute Temperature. Application a la Thermolyse de l'Eau**, The Canadian Journal of Chemical Engineering, Vol.63, June 1985.

[21] J.L. Houzelot, J.Villermaux, **A Novel Device for Quenching The Cylindrical Annular Exchanger in Laminar Flow**, Chemical Engineering Science, Vol.39, No.9, pp.1409-1413.

[22] F.Lapique, J.Lede,P.Tironneau, J.Villermaux, **A Solar Reactor for High-Temperature Gas Phase Reactions(Water and Carbon Dioxide Thermolysis and Nitric Oxide Synthesis**, Solar Energy, Vol. 35, No.2, pp.153-166, 1985.

[23] F.Lapique, J.Lede, J.Villermaux, **Design and Optimization of a Reactor for High Temperature Dissociation of Water and Carbon Dioxide Using Solar Energy**, Chemical Engineering Science, Vol.41, pp.677-684, 1986.

[24] B. Cheynet, **Recherche et optimisation thermodynamique d'un cycle thermochemique de decomposition de L'eau**, These, Grenoble (September 1978).

[25] J. Falley, **Hydrogen Generating Device**, Belgian Patent No. 845,009, Assigned to Compagnie Generale d'Electricite, February 9, 1977.

[26] R. Bidard, V. La Roche, **Modern Technology Electrolysis for Power Application**, World Hydrogen Energy Conf. No. 1, 7B-53 to 7B-75, 1976.

[27] R.Diver, E.A. Fletcher, **Thoria effusion membranes**, Am.Ceramic Soc. Bull. 56, 1019 (1977).

[28] D.E. Monahan, **Process and Apparatus for Generating Hydrogen and Oxygen using Solar Energy**, U.S. Patent No. 4,233,127, November 11, 1980.

[29] R.L. Curl, **Direct Thermo-magnetic Splitting of Water**, Int.Jour.Hydrogen Energy, Vol.4, pp.13-20, 1979.

[30] R.E. Diggs, **Solar Power System**, U.S. Patent No. 4,030,890, June 21, 1977.

[31] H.H.G. Jellinek, H. Kachi, **The Catalytic Thermal Decomposition of Water and the Production of Hydrogen**, Int. Journ.Hydrogen Energy, Vol.9, No.8, pp.667-688, 1984.

[32] W.R. Pyle, **Photo-separatory Nozzle**, U.S. Patent No. 4,405,594, Assigned to Chevron Research Center, September 20, 1983.

[33] R.B. Diver, D.E.E. Carlson, F.J. McDonald, E.D. Fletcher, J. Solar Energy Eng. 105, 291 (1983).

[34] E.M. Sparrow, V.K. Jonsson, **Absorbtion and emission characteristics of diffuse spherical enclosures**, NASA TN D-1289 (1962).

[35] E.A. Fletcher, R.L. Moen, **Hydrogen and Oxygen from Water, the Use of Solar Energy in a one-step Effusional Process is Considered**, Science, Vol.197, pp.1050-1056, September 1977.

[36] D. Sebacher, A.P. Sabol, **Solar Hydrogen Generator**, U.S. Patent 4, 019,868, Assigned to NASA Washington D.C. April 26, 1977.

[37] E. Bilgen, **On the feasibility of direct dissociation of water using solar energy**, Technical Report EP-75-R-10, 75510, Ecole Polytechnique, Montreal, Canada, pp.16 (February 1975).

[38] E. Bilgen, M. Ducarroir, M. Foex, F. Sibieude, F. Trombe, **Use of solar energy for direct two-step water decomposition cycles**, Int.J. Hydrogen Energy, 2, 251 (1977).

[39] E. Bilgen, **Thermodynamics of one and two-step thermochemical cycles**, Tech.Report Ecole Polytechnique, Montreal, Canada (August 1978).

[40] C. Bilgen, E. Bilgen, **Solar Synthetic Fuel Production**, Int.J. Hydrogen Energy, Vol.6, pp. 349-362, 1981.

[41] E. Bilgen, J.P.Bourquin, **Solar power plants**, Proc. Renewable Alternatives 1978 Conference, SESCI, Univ.Western Ontario (1978).

[42] E. Bilgen, J.Galindo, **High Temperature Solar Reactors for Hydrogen Production**, Int. J. Hydrogen Energy, Vol.6, pp.139-152, (1981).

[43] S.Z. Baykara, E. Bilgen, **An Overall Assessment of Hydrogen Production by Solar Water Thermolysis**, Int.J. Hydrogen Energy, Vol.14, No.12, pp.881-891, (1989).

[44] E. Meirovitch, A.Segal, M.Levy, **Theoretical Modeling of a Directly Heated Solar-Driven Chemical Reactor**, Solar Energy Vol.45, No.3, pp.139-148, (1990).

[45] I.Hodara, A. Kogan, A. Grodnev, **Direct Solar Water Splitting Experiment**, Proc.Project Hydrogen 91, American Academy of Science, pp.125-135, 1992.

[46] A. Kogan, **Separation of a Gas Mixture in Curved Supersonic Flow**, Int.J.Heat Transfer, Vol.9, p.1-10, Pergammon Press, 1966.

[47] S. Ihara, **Feasibility of Hydrogen Production by Direct Water Splitting at High Temperature**, Proc. World Hydrogen Energy Conf. No.1, 5b-55 to5b-78, 1976.

[48] S. Ihara, **On the Study of Hydrogen Production from Water Using Solar Thermal Energy**, Int.J. Hydrogen Energy, Vol.5, pp.527-534, 1980.

[49] T. Nakamura, **An Investigation of Hydrogen Production from Water at High Temperatures**, World Hydrogen Energy Conf. No1, pp.5b-77 to 5b-96, 1976.

[50] K.L. Coulson, **Solar and Terrestrial Radiation**, Academic Press, p.40, 1975.

[51] D.P. DeWitt, G.D. Hutter, **Theory and Practice of Radiation Pyrometry**, John Wiley & Sons, p.207, 1988.

[52] ibid, p.207

[53] Ibid, p.42

[54] G. Hertz, Z. Phys. 79, 108 (1932).

[55] E.W. Becker, K. Bier, Z. Naturforschg. 9a, 975 (1954)

[56] Becker, E.W., Bier K., Burghoff, H. **"The Separatory Nozzle a New Device for Separation of Gases and Isotopes"**, Z. Naturforschg.,part A Vol.10 a,1955, pp. 565-572.

[57] Becker, E.W., Bier, W., Ehrfeld, W., Eisenbeiss , G., Frey, G., Geppert, H., Happe, P., Heeschen, G,.Lucke, R., Plesch, D., Schubert, K., Schutte, R., Seidel, D., Sieber, U., Volcker, H., Weis, F., **"The Separation Nozzle Process For Enrichment of U 235"** ., U.N. International Conference on the Peaceful Uses of Atomic Energy; A/Conf. 49/P383 (Geneva) 1971.

[58] Becker, E.W., Bier, W., Fritz, W., Happe, P., Plesch, D., Schubert, K., Schutte, R., Seidel, D., **"Current Status of the Separation Nozzle Technology"**, International Conference on Uranium Isotope Separation (London 1975).

[59] Becker, E.W., Berkhahn, W.,Bley ,P., Ehrfeld, U., Ehrfeld, W., Knapp, U., **"Physics and Development Potential of the Separation Nozzle Process"**, International Conference on Uranium Isotope Separation (London 1975).

[60] Becker, E.W., Bier, W., Ehrfeld, W., Schubert, K., Schutte, R., Seidel, D.**, "Physics and Technology of Separation Nozzle Process"**, Nuclear Energy Maturity :Proceedings of the European Nuclear Conference, Paris, April 21-25, 1975, Volume 12, pp. 44-52.

[61] Becker, E.W., **"Process for Separating Gaseous or Vaporous Substances, Especially Isotopes"**, United States Patent no. 3,362,131, filed March 9, 1964, assigned to Gesellschaft Fur Kernforschung M.B.H., Karlsruhe, Germany, Patented January 9, 1968.

[62] Becker. E.W., Bley, P., Ehrfeld, W., Ehrfeld, U., Krieg, G., **"Separation of Gaseous or Vaporous Substances According to the Separating Nozzle Principle"**, United States Patent no. 4,246,007, filed Dec.6, 1978, assigned to Kernforschungszentrum Karlsruhe, Karlsruhe, Germany Patented January 20,1981.

[63] Geppert , H., Schumann, P. , Sieber, U., Stermann, H. P. , Volcker, H., Weinhold, G., **"The Industrial Implementation of the Separation Nozzle Process"**, British Nuclear Energy Society , London, 1976, pp. 17-26.

[64] Fisher , S.S., Knuth, E.L., **"Properties of Low-Density Free Jets Measured Using Molecular Beam Techniques"**, AAIA Journal, Vol. 7, no.6 1969, pp. 1174-1177.

[65] Bier K., Hagena O. **"Optimum Conditions for Generating Supersonic Molecular Beams"**, Rarified Gas Dynamics, Edited by J.H. De Leeuw, Vol. 2, Academic Press, New York, 1966., pp. 260-278.

[66] Miller, D.R. , Andres, R.P. **"Rotational Relaxation of Molecular Nitrogen"**, Journal of Chemical Physics, Vol. 46, no.9, May 1967 , pp. 3418-3423.

[67] Scott, J. E. Jr. , Phipps, J.A. **"Translational Freezing in Freely Expanding Jets"**, Rarified Gas Dynamics, Edited by C. L. Brundin, Vol.2 Academic Press, New York, 1967 pp. 1337-1352.

[68] McMichael, G.E., French, J.B. **"Electron Beam Studies of Skimmer Interaction in a Free Jet "**, Physics of Fluids, Vol. 9 1966, pp. 1419-1420.

[69] Bird, G.A. **"Chemically Reacting Gas Flows"**, Chapter 12 of Molecular Gas Dynamics, Clarendon Press, Oxford, 1976.

[70] Wakuta, Y., Koga, Y., Hasuyama, H., Yamamoto, H., **"Effect of Dissociator-Nozzle Temperature on Polarized Atomic Hydrogen Beam Intensities"**, Nuclear Instruments and Methods 147 (1977), pp. 461- 463.

[71] Field, J.E., JR. Poldervaart, L.J., Wijnands, P.J., **"A Photographic Study of the Interaction of Two High-Velocity Gas Jets"**, Spie Vol. 97, High Speed Photgraphy, Toronto, 1976.

[72] Bossel, U., **"On the Optimization of Skimmer Geometries"**, Entropie, No.42, November-December 1971.

[73] Bossel ,U. , **"Skimming of Molecular Beams from Diverging Non-Equilibrium Gas Jets"**, Archives of Mechanics, Vol. 26, pp. 355-367, Warszawa, 1974.

[74] Molmud, P., **"Expansion of a Rarified Gas Cloud into a Vacuum"**, Physics of Fluids, Vol.3 no.3, May - June , 1960.

[75] Bossel, U., Hurlbut, F.C., Sherman, F.S. **"Extraction of Molecular Beams from Nearly - Inviscid Hypersonic Free Jets"** , Rarified Gas Dynamics: Proceedings of 6th International Symposium, edited by L. Trilling and H. Wachman, Vol.II , Academic Press, New York, 1968, pp. 945-964.

[76] Bird, G.A. , **"Transition Regime Behavior of Supersonic Beam Skimmers"**, Physics of Fluids, Vol. 19, no. October, 1976.

[77] Greenberg, R.A. , Schneiderman, A.M., Ahouse,D.R., Parmentier, E.M. **"Rapid Expansion Nozzles for Gas Dynamic Lasers"**, AIAA Journal, Vol.10 no. 11 November 1972, pp. 1494-1498.

[78] Niemann, H.J. , Sprehe, J. **"Separating Components of Different Masses in a Gas Flow"**, UK Patent Application GB 2,037,610A, Filed 19 Nov 1979, Published 16 July 1980.

[79] Bley P., Ehrfeld, W., Eisenbeiss, G. **"Separation of Fluid Substances"**, United States Patent no. 3,877,892, filed Sept. 6,1973,assigned to Gesellschaft Fur Kernforschung M.B.H., Karlscruhe, Germany, Patented April 15, 1975.

[80] Fenn, J.B. , **"Separation of Components from Gaseous Streams"**, Canadian Patent no. 916,065, filed July 28, 1969, assigned to Mobil Oil Company, New York , U.S.A. Issued Dec. 5, 1972.

[81] H. Dun, B.L. Mattes, D.J. Stevenson, **"The Gas Dynamics of a Conical Nozzle Molecular Beam Sampling System"**, Chemical Physics 38, pp.161-172, (1979).

[82] B.F.J. Schonland, **"Atmospheric Electricity"**, Methuen, London (1953).

[83] E. Kuffel, Proceedings IEE 106C, 133 (1959).

[84] E. Pfender, (Edited by M.N. Hirsh, H.K. Oskam), **"Electric Arcs and Arc Gas Heaters"**, Gaseous Electronics Vol.1, Chapter 5, pp.293-295, Academic Press (1978).

[85] ibid, J.H. Ingold, Chapter 2, **"Glow Discharges at DC and Low Frequencies"**, pp.19-20.

86 ibid, pp.21-22.

87 ibid, pp.23-27.

88 ibid, pp.133-170.

89 J.D. Cobine, **"Gaseous Electronics"**, Chapters V, VI, VII, IX, Dover, New York, 1958.

90 R. Botter, H.M. Rosenstock, **"Franck-Condon Factors for the Ionization of H2O and D2O"**, J. Research., Nat. Bur. Stand., A: Physics & Chem., Vol. 73A, No.3, May-June, 1969.

91 G.R. Branton, C.E. Brion, **"Total Absorption and the Energy Dependence of the Partial Oscillator Strengths for :Photoionization of the Valence Orbitals of H2O using an Electron-Electron Coincidence Method"**, J. Electron Spectroscopy and Related Phenomena, 3, p.129-135, 1974.

92 C.E. Melton, **"Cross Sections and Interpretation of Dissociative Attachment Reactions Producing OH^-, O^-, and H^- in H_2O^{*}"**, J.Chem.Physics, Vol.57, No.10, Nov. 1972.

93 P.F. Knewstubb, A.W. Tickner, **"Mass Spectrometry of Ions in Glow Discharges IV Water Vapor"**, J.Chem. Physics, Vol. 38, No.2, Jan. 1963.

94 P.A. Lehman , C.E. Chamberlin, G. Pauletto, M.A. Rocheleau, **Operating Experience With a Photobvoltaic-Hydrogen Energy System**, Hydrogen Energy Progress X-Proceedings oth the 10th World Hydrogen Energy Conference, Cocoa Beach Florida, USA, June 20-24 1994, Vol 1. pp.411-420.

95 F. Rosa, E. Lopez, A.G. Garcia-Conde, R. Luque, F. del Pozo, **Intermittant Operation of a Solar Hydrogen Production Facility: Yearly Evaluation**, Hydrogen Energy Progress X-Proceedings oth the 10th World Hydrogen Energy Conference, Cocoa Beach Florida, USA, June 20-24 1994, Vol 1. pp.421-430.

96 H. Braun, **The Phoenix Project-An Energy Transition to Renewable Sources**, Research Analyst, Phoenix AZ, 1990, pp.184-194.

97 W.R Pyle personal communications with Dr. L.M. Fraas, Boeing Co, Seattle WA, March 1991.

98 Kent Scholl, **"Proceedings of the 1994 DOE/NREL Hydrogen Program Review April 18-21, 1994 Livermore, California"**, U.S. Dept of Energy National Renewable Energy Laboratory Golden Colorado July 1994, pp. 291-299.

99 S.V. Korobtsev, T.A. Kosinova, B.V. Potapkin, Y.R. Rakhimbabaev, V.D. Rusanov, A.A. Fridman, E.V. Shulakova, **"The Centrifugal Effect in the Kinetics of the Water Dissociation**

Process in Rotating Plasma", Kurchatov Ins. Atomic Energy, Proc. World Hydrogen Energy Conf. No.2, pp. 1071-1077.

100 J.L. Wiza, **"The Microchannel Plate a Shift to Ill and New Terrain"**, Optical Spectra, pp. 58-62, April, 1981.

101 K. Kawata, T. Sato, T. Mizutani, Matsushita Electric Ind. Co., **"Electric Discharge Machine for Precise Machining of Microholes"** , Model MG-ED01, Research and Development, p.84, Oct. 1985.

102 N.J. Freundlich, **"Microtip TV,"** Popular Science, pp. 60-89, Aug. 1987.

103 D.L. Wells, **"Making Nozzles from Hard Material"**, NASA Tech Briefs, p.71,Nov. 1989.

104 H. Gray, **"New Device Combines Advantages of Vacuum and Solid State Technology"**, Nav. Res. Lab. Wash. D.C. , Research and Development Research Trendletter.

105 Metrigraphics Div. Dynamics Res. Corp., Wilmington Mass. **"Precision Electroforming - 2um Holes in Metal"**.